Semiclassical theory of nonlinear magneto-optical responses with applications to topological Dirac/Weyl semimetals

Takahiro Morimoto,[1,*] Shudan Zhong,[1] Joseph Orenstein,[1,2] and Joel E. Moore[1,2]
[1]*Department of Physics, University of California, Berkeley, Berkeley, California 94720, USA*
[2]*Materials Sciences Division, Lawrence Berkeley National Laboratory, Berkeley, California 94720, USA*
(Received 19 September 2016; revised manuscript received 22 November 2016; published 16 December 2016)

We study nonlinear magneto-optical responses of metals by a semiclassical Boltzmann equation approach. We derive general formulas for linear and second-order nonlinear optical effects in the presence of magnetic fields that include both the Berry curvature and the orbital magnetic moment. Applied to Weyl fermions, the semiclassical approach (i) captures the directional anisotropy of linear conductivity under a magnetic field as a consequence of an anisotropic B^2 contribution, which may explain the low-field regime of recent experiments; and (ii) predicts strong second harmonic generation proportional to B that is enhanced as the Fermi energy approaches the Weyl point, leading to large nonlinear Kerr rotation. Moreover, we show that the semiclassical formula for the circular photogalvanic effect arising from the Berry curvature dipole is reproduced by a full quantum calculation using a Floquet approach.

DOI: 10.1103/PhysRevB.94.245121

I. INTRODUCTION

The wave function of a single electron moving through a crystal has several geometric properties whose importance in insulators is well known. The most celebrated example is the Berry phase derived from Bloch states. It gives a gauge field in momentum space that underlies topological phases ranging from the integer quantum Hall effect to topological insulators. These phases are characterized by topological invariants that can be expressed as integrals of Berry gauge fields; even in ordinary insulators, similar integrals describe important physical quantities such as electric polarization [1,2] as well as the magnetoelectric response [3–6].

In metals, the Berry gauge field is known to give an additional term (the "anomalous velocity") in the semiclassical equations of motion that describe the motion in real and momentum space of a wave packet made from Bloch states. The anomalous velocity was originally discussed in the context of the anomalous Hall effect in magnetic metals such as iron. The semiclassical equations can be derived systematically to linear order in applied electric and magnetic fields, under certain assumptions that we review more fully in Sec. II. In several cases, such as the anomalous Hall effect [7] and the gyrotropic or "transport limit" of the chiral magnetic effect [8,9], the semiclassical approach (SCA) fully reproduces the results obtained from quantum mechanical calculations based on the Kubo formula.

The focus of this paper is the semiclassical theory of *nonlinear* properties of metals that are currently active subjects of experimental and theoretical investigation. One motivation is that systematic quantum mechanical derivations that capture all contributions to a given nonlinear order in applied fields have not as yet been achieved. An example we consider is the chiral anomaly, which in a solid is a particular type of angle-dependent magnetoresistance (MR) with an enhanced electrical conductivity along the direction of an applied magnetic field. This effect has been argued to exist based on linearization near isolated Dirac or Weyl singularities, but the lesson of the past few years of work on the chiral magnetic effect is that it can be dangerous to treat the singularities solely and without including all effects at a given order. We derive a semiclassical formula for magnetotransport in the weak-field regime of this problem and discuss that including all terms gives an answer distinct from that in other recent work, which may explain experimental observations on a Dirac semimetal in this regime [10,11].

The semiclassical equations of motion for an electron wave packet in a metal are [12]

$$\dot{\boldsymbol{r}} = \frac{1}{\hbar}\nabla_{\boldsymbol{k}}\epsilon_{\boldsymbol{k}} - \dot{\boldsymbol{k}} \times \boldsymbol{\Omega}, \tag{1a}$$

$$\hbar\dot{\boldsymbol{k}} = -e\boldsymbol{E} - e\dot{\boldsymbol{r}} \times \boldsymbol{B}. \tag{1b}$$

One new contribution compared to the version in older textbooks [13] is from the Berry curvature in momentum space,

$$\Omega = -\mathrm{Im}[\langle\nabla_{\boldsymbol{k}} u_{\boldsymbol{k}}| \times |\nabla_{\boldsymbol{k}} u_{\boldsymbol{k}}\rangle], \tag{2}$$

and another is from the orbital magnetic moment contribution to the energy dispersion, $\epsilon_{\boldsymbol{k}} = \epsilon^0_{\boldsymbol{k}} - \boldsymbol{m}_{\boldsymbol{k}} \cdot \boldsymbol{B}$, where $H_{\boldsymbol{k}}|u_{\boldsymbol{k}}\rangle = \epsilon^0_{\boldsymbol{k}}|u_{\boldsymbol{k}}\rangle$ with $B = 0$ and the orbital magnetic moment is

$$\boldsymbol{m}_{\boldsymbol{k}} = -\frac{e}{2\hbar}\mathrm{Im}\big[\langle\nabla_{\boldsymbol{k}} u_{\boldsymbol{k}}| \times \big(H_{\boldsymbol{k}} - \epsilon^0_{\boldsymbol{k}}\big)|\nabla_{\boldsymbol{k}} u_{\boldsymbol{k}}\rangle\big]. \tag{3}$$

(We note that we adopt the convention $e > 0$.)

These equations conserve the properly defined volume in phase space and give an intuitive approach to many observable properties of metals. However, the SCA can make erroneous predictions if used outside the regime of its validity. To illustrate this point we present, in Sec. II, the predictions of semiclassical and fully quantum theories of a fundamental nonlinear response in metals with a low symmetry: the photogalvanic effect (PGE) [14–16]. The term "photogalvanic" refers to the generation of a dc current by a time-varying electric field, with the amplitude proportional to the square of the applied field. The PGE is distinguished from a conventional photovoltaic response by the dependence of the dc current on the polarization state of the electric field.

*tmorimoto@berkeley.edu

 ©2016 American Physical Society

For example, in the the circular PGE (CPGE) the direction of the dc current reverses when the polarization state of the time-varying field is changed from left to right circular. Using the SCA the CPGE has been shown to have a Berry-phase contribution [17] in two-dimensional and, more recently, in three-dimensional [18] systems such as Weyl semimetals.

In Sec. II we show that the previous semiclassical predictions for the CPGE can be derived in a fully quantum theory by using the Floquet approach [19]. We first derive the Berry curvature formula for CPGE in the case of two bands and then generalize the derivation to the cases with many bands. This indicates that the CPGE provides a good example where the nonlinear effects that follow from semiclassical equations are exactly what is obtained from a full quantum derivation, which was previously only known in the linear case. We also show that in this same limit in which interband terms are neglected, there is a close quantitative relation between the CPGE and second-harmonic generation (SHG).

In Sec. III we derive semiclassical formulas for a variety of nonlinear effects. In particular, we systematically study nonlinear magneto-optical effects by incorporating the orbital magnetic moment, which has not been discussed previously. We show that magnetic fields modify the nonlinear Hall effect via the orbital moment of Bloch electrons. In Sec. IV, we apply our semiclassical formula to magnetotransport of Weyl/Dirac semimetals and study the angle-dependent MR. We find that there exist contributions of opposite sign from the orbital magnetic moment and Berry curvature in addition to the contribution of the chiral anomaly. The angular dependence that we obtain by taking into account all the contributions at the same order in the SCA is compared with recent magnetotransport experiments [10,11]. Section V applies the semiclassical formulas to nonlinear Kerr rotation (polarization rotation of SHG signals with applied magnetic fields) of Weyl semimetals. Since isotropic Weyl fermions with linear dispersion support no intraband contribution to SHG in the absence of magnetic fields, intraband contributions to SHG in such Weyl semimetals are linear in B, which leads to nonlinear Kerr rotation in general. We show that Weyl semimetals can exhibit giant nonlinear Kerr rotation in the infrared regime as the Fermi energy approaches the Weyl points. Section VI summarizes some remaining issues and open problems.

II. NONLINEAR OPTICAL EFFECTS AND FLOQUET APPROACH

In this section, we first review formulas for the nonlinear Kerr rotation and CPGE. Previous works based on SCA showed that those nonlinear optical effects are described by a geometrical quantity, i.e., the Berry curvature dipole [18]. We give an alternative derivation for those formulas based on fully quantum theoretical treatment by applying the Floquet formalism for a two-band system.

A. Geometrical meaning of nonlinear optics in the semiclassical approach

In previous semiclassical works [17,18], it has been shown that the intraband contributions to SHG and CPGE have a geometrical nature that is described by Berry curvatures of Bloch wave functions. The SHG is the second-order nonlinear optical effect, which is described by nonlinear current responses $\boldsymbol{j}(2\omega)e^{-2i\omega t}$ as

$$j_a^{(2\omega)} = \sigma_{abc} E_b E_c, \tag{4}$$

where the external electric field is given by

$$\boldsymbol{E}(t) = \boldsymbol{E} e^{-i\omega t} + \boldsymbol{E}^* e^{i\omega t}. \tag{5}$$

The nonlinear Hall effect in Ref. [18] refers to a transverse current response that is described by σ_{abb} with $a \neq b$. Similarly, the CPGE is the second-order nonlinear optical effect in which the dc photocurrent of $\boldsymbol{j}^{(0)}$ is induced by circularly polarized light as

$$j_a^{(0)} = \sigma_{abc} E_b E_c^*. \tag{6}$$

In a time reversal (TR)-symmetric material, these nonlinear response tensors σ are given by

$$\sigma_{abc} = \epsilon_{adc} \frac{e^3 \tau}{\hbar(1 - i\omega\tau)} \int [d\boldsymbol{k}] f_0 (\partial_b \Omega_d), \tag{7}$$

where the frequency ω is much smaller than the resonant frequency for optical transitions (i.e., the intraband contribution). Here, ϵ_{abc} is the totally antisymmetric tensor, f_0 is the Fermi distribution function, and we have used the notation $[d\boldsymbol{k}] = d\boldsymbol{k}/(2\pi)^d$ with the dimension d.

We focus here on the case of a three-dimensional material [18] but have adopted notations for $\boldsymbol{E}(t)$ and j slightly different from those in Ref. [18], which results in a modified expression for σ above. While these nonlinear effects are Fermi surface effects because one obtains $\sigma_{abc} \propto \epsilon_{adc} \int [d\boldsymbol{k}] (\partial_b f_0) \Omega_d$ by integrating by parts, they can also be understood as currents carried by electrons in the Fermi sea with an anomalous velocity originating from the Berry curvature dipole.

The way in which the anomalous velocity ($\dot{\boldsymbol{k}} \times \boldsymbol{\Omega}$) of electron wave packets driven by an external electric field leads to the CPGE and SHG is schematically illustrated in Fig. 1. Circular polarized light induces circular motion of the wave packet in momentum space [Fig. 1(a)]. In the presence of the Berry curvature dipole, the anomalous velocities in regions with $\Omega > 0$ and $\Omega < 0$ add up, which results in a dc current. Similarly, linearly polarized light induces an oscillation of the wave packet as shown in Fig. 1(b). The driven wave packet exhibits anomalous velocities in the y direction that oscillate twice in the driving period, which results in SHG.

B. Fully quantum mechanical derivation by the Floquet formalism

Systematic derivations for nonlinear optical effects including the CPGE and SHG are presented in Sec. III using the SCA for general cases with a finite $\boldsymbol{B}$. Before proceeding to a general discussion of $\boldsymbol{B}$, we study these nonlinear optical effects from a fully quantum mechanical treatment using a two-band model. The focus of interest is whether the fully quantum mechanical expression coincides with the semiclassical formula. While the SCA partially includes high-energy bands through Ω, it does not necessarily capture all effects of the high-energy bands. Thus it is an interesting question whether the geometrical formulas for the CPGE and SHG hold even in the fully quantum mechanical treatment. In the following, we study the

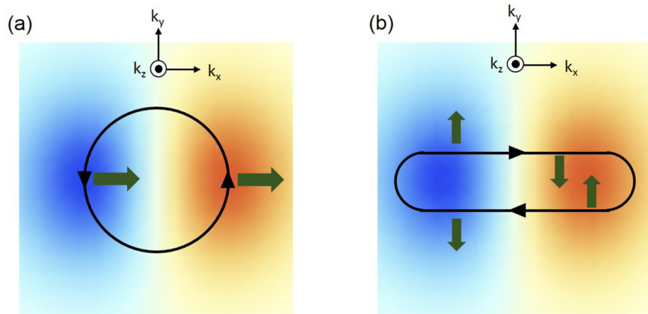

FIG. 1. Semiclassical picture of CPGE and SHG induced by a Berry curvature dipole. The distribution of Berry curvature in momentum space is indicated by the color scale, with the red region corresponding to $\Omega_z > 0$ and the blue region to $\Omega_z < 0$. (a) CPGE arises from circular motion of the electron wave packet in momentum space driven by circularly polarized light. The dipole structure in $\Omega(k)$ induces an anomalous velocity $(\dot{\boldsymbol{k}} \times \boldsymbol{\Omega})$ in the x direction denoted by green arrows. (b) SHG arises from oscillation of the electron wave packet driven by linearly polarized light in the x direction. The Berry curvature dipole leads to an anomalous velocity that undergoes two oscillations in the y direction in one driving period. The configuration of Berry curvature shown preserves C_{2v} point-group symmetry (which is present for typical polar crystals that support CPGE and SHG), where the y axis corresponds to the polar axis and the yz plane to the mirror plane.

intraband contribution to the CPGE and SHG by applying the Floquet formalism and show that the Berry curvature formula is indeed exact in the fully quantum mechanical treatment.

First, we study a two-band system periodically driven by an external electric field using the Floquet formalism (for details of the Floquet formalism, see Refs. [19–21]. When the original Hamiltonian of the two-band system is given by a Bloch Hamiltonian, $H_{\text{orig}}(k)$, the time-dependent Hamiltonian of the system driven by $E(t) = Ee^{-i\omega t} + E^* e^{i\omega t}$ is given by

$$H(t,k) = H_{\text{orig}}(k + eA(t)), \tag{8}$$

$$A(t) = i\frac{E}{\omega}e^{-i\omega t} - i\frac{E^*}{\omega}e^{i\omega t}, \tag{9}$$

which is periodic in time with $t \to t + 2\pi/\omega$. For such periodically driven systems, the Floquet formalism gives a concise description in terms of the band picture as follows. The Floquet formalism is, roughly speaking, a time-direction analog of Bloch's theorem for the time-dependent Hamiltonian $H(t)$ that satisfies $H(t+T) = H(t)$ with period T. Namely, in a similar manner to Bloch's theorem, the solution for the time-periodic Schrödinger equation,

$$i\hbar\frac{\partial\psi(t)}{\partial t} = H(t)\psi(t), \tag{10}$$

is given by a time-periodic form,

$$\psi(t) = e^{-i\epsilon t/\hbar}\phi(t), \quad \phi(t+T) = \phi(t), \tag{11}$$

with the quasienergy ϵ. Using the time-periodic part of the wave function $\phi(t)$, the time-dependent Schrödinger equation is rewritten as

$$(i\hbar\partial_t + \epsilon)\phi(t) = H(t)\phi(t). \tag{12}$$

Since $\phi(t)$ is periodic in time, we can perform Fourier transformation of both sides with

$$\phi(t) = \sum_m e^{-im\omega t}\phi_m \tag{13}$$

and obtain

$$(m\hbar\omega + \epsilon)\phi_m = \widetilde{H}_{mn}\phi_n, \tag{14}$$

$$\widetilde{H}_{mn} = \frac{1}{T}\int_0^T dt e^{i(m-n)\omega t}H(t). \tag{15}$$

Here $\widetilde{H}_{mn}$ is time independent but has an additional matrix structure spanned by Floquet indices m and n. Thus the time-dependent Schrödinger equation effectively reduces to a time-independent one in the Floquet formalism as

$$H_F\phi = \epsilon\phi, \tag{16}$$

where the Floquet Hamiltonian is given by

$$(H_F)_{mn} = \frac{1}{T}\int_0^T dt e^{i(m-n)\omega t}H(t) - n\hbar\omega\delta_{mn}. \tag{17}$$

Floquet bands obtained by diagonalizing the Floquet Hamiltonian H_F offer a concise understanding of the dynamics of a driven system in terms of an effective band picture. We note that the energy spectrum of ϵ shows a periodic structure with $\hbar\omega$ as a consequence of the translation symmetry with respect to the Floquet index n. Thus the quasienergy spectrum is essentially described within the range $-\hbar\omega/2 \leqslant \epsilon < \hbar\omega/2$, which is an analog of "the first Brillouin zone" (BZ) in Bloch's theorem.

Since we consider the case of a driving frequency much lower than the band gap, we can obtain the current expectation value by studying the Floquet band that is connected to the valence band in the undriven system. In order to do so, we use standard second-order perturbation theory for

$$H_F = H_0 + H_1 + H_2, \tag{18}$$

where H_i represents a term in the Floquet Hamiltonian proportional to A^i. The wave function up to the second order in A reads

$$\begin{aligned}|\psi_n\rangle = |n\rangle &- \sum_{m\neq n}\frac{(H_1)_{mn}}{E_m - E_n}|m\rangle \\ &\times \sum_{m\neq n}\Bigg[-\frac{(H_2)_{mn}}{E_m - E_n} - \frac{(H_1)_{mn}(H_1)_{nn}}{(E_m - E_n)^2} \\ &+ \sum_{k\neq n}\frac{(H_1)_{mk}(H_1)_{kn}}{(E_m - E_n)(E_k - E_n)}\Bigg]|m\rangle,\end{aligned} \tag{19}$$

where $H_0|n\rangle = E_n|n\rangle$. By applying the above formula to the Floquet Hamiltonian H_F, we obtain Floquet states $|\psi\rangle$ that describe the steady state under the drive of incident light. The current responses in the steady state are obtained from perturbed Floquet states that are connected to the original valence bands. This treatment can be justified when the frequency of incident light is much lower than the energy difference between valence and conduction bands. (When ω satisfies the conditions for optical resonances, Floquet bands originating from valence and conduction bands anticross each other. In this case, we cannot naively determine the occupation of resulting Floquet bands, which requires considering the coupling to a heat bath [19].)

Using the Floquet state $|\psi\rangle$ connected to the valence band, the time-dependent current in the steady state is given by

$$J_\alpha(t) = \sum_{m,n} \{\mathrm{tr}[|\psi\rangle\langle\psi|\hat{v_\alpha}]\}_{mn} e^{-i(m-n)\omega t}, \tag{20}$$

where tr denotes the trace over the band index, m and n are Floquet indices, and $\hat{v_\alpha}$ is the current operator along the α direction, given by

$$(\hat{v_\alpha})_{mn} = \frac{1}{T}\int_0^T dt e^{i(m-n)\omega t}\frac{\partial H(t)}{\partial k_\alpha}. \tag{21}$$

In the following, we derive representative components of the nonlinear response tensor describing the CPGE and SHG using the above method.

To study the CPGE we consider a system subjected to the left circularly polarized light in the xy plane, where the electric field is given by

$$\boldsymbol{E}(t) = E(\boldsymbol{e_x} + i\boldsymbol{e_y})e^{-i\omega t} + E^*(\boldsymbol{e_x} - i\boldsymbol{e_y})e^{i\omega t}. \tag{22}$$

In this case, the Floquet Hamiltonian is written as

$$H_F = H_0 + H_1, \tag{23}$$

$$(H_0)_{mn} = \begin{pmatrix} \epsilon_v - n\omega & 0 \\ 0 & \epsilon_c - n\omega \end{pmatrix}\delta_{mn}, \tag{24}$$

$$(H_1)_{mn} = -iA^*(v_x - iv_y)\delta_{mn-1} + iA(v_x + iv_y)\delta_{mn+1}, \tag{25}$$

where $\epsilon_{v/c}$ is the energy of the valence/conduction band, $v_i = \partial H_0/\partial k_i$ is the velocity operator for the static Hamiltonian, $A = E/\omega$, and we set $e = 1, \hbar = 1$ for simplicity. Here we have dropped the term H_2 proportional to A^2 because it does not contribute to the dc photocurrent, which is proportional to AA^* and does not involve A^2 terms in the end. Since we are interested in the second-order nonlinear current responses, it is sufficient to consider the Floquet Hamiltonian with $n = -2, \ldots, 2$ by starting with the unperturbed wave function $|\psi_{\mathrm{ini}}\rangle = |u_{v,n=0}\rangle$. Now we study the dc current in the x direction induced by circularly polarized light for the steady state described by the Floquet state in Eq. (19). The velocity operator in the x direction is written up to linear order in A as

$$\begin{aligned}\hat{v_x} &= v_x\delta_{mn} - iA^*\partial_{k_x}(v_x - iv_y)\delta_{mn-1} \\ &\quad + iA\partial_{k_x}(v_x + iv_y)\delta_{mn+1}.\end{aligned} \tag{26}$$

Using Eq. (20), we obtain the CPGE photocurrent $J_x = \int [d\boldsymbol{k}] j_x^{(0)}$ as

$$\begin{aligned} j_x^{(0)} &= \sum_n \{\mathrm{tr}[|\psi\rangle\langle\psi|\hat{v_x}]\}_{nn} \\ &= 4\frac{|E|^2}{\omega}\left\{\frac{\mathrm{Im}[(\partial_{k_x}v_x)_{vc}(v_y)_{cv} + (v_x)_{vc}(\partial_{k_x}v_y)_{cv}]}{(\epsilon_v - \epsilon_c)^2}\right. \\ &\quad \left. -3\frac{\mathrm{Im}[(v_x)_{vc}(v_y)_{cv}][(v_x)_{vv} - (v_x)_{cc}]}{(\epsilon_v - \epsilon_c)^3}\right\}, \end{aligned} \tag{27}$$

where we have dropped higher order terms with respect to ω by focusing on the current response in the low-frequency limit. We note that the contributions proportional to $|E|^2/\omega^2$ vanish due to the time reversal symmetry (TRS; e.g., the TRS $T = \mathcal{K}$ constrains Re[v] and Im[v] to be odd and even functions of k, respectively), which is used when going from the first line to the second line. In the case of two-band models, the Berry curvature is written as

$$\Omega_z = -\frac{2\mathrm{Im}[(v_x)_{vc}(v_y)_{cv}]}{(\epsilon_v - \epsilon_c)^2}, \tag{28}$$

and the matrix elements of $\partial_{k_i} v_j$ can be rewritten as

$$\begin{aligned}\left(\partial_{k_i} v_j\right)_{vc} &= \partial_{k_i}[(v_j)_{vc}] + (v_j)_{vc}[i(a_i)_v - i(a_i)_c] \\ &\quad + (v_i)_{vc}\frac{(v_j)_{vv} - (v_j)_{cc}}{\epsilon_v - \epsilon_c},\end{aligned} \tag{29}$$

with $(a_i)_{v/c} = \langle u_{v/c}|\partial_{k_i}|u_{v/c}\rangle$. Using these formulas, the CPGE photocurrent can be further reduced as

$$j_x^{(0)} = 4\frac{|E|^2}{\omega}\frac{\partial}{\partial k_x}\left[\frac{\mathrm{Im}[(v_x)_{vc}(v_y)_{cv}]}{(\epsilon_v - \epsilon_c)^2}\right] = -2\frac{|E|^2}{\omega}\partial_{k_x}\Omega_z. \tag{30}$$

The nonlinear conductivity tensor is obtained by equating the above expression and j_x in terms of σ and $\boldsymbol{E}(t)$ [in Eq. (22)], given by

$$j_x = -i\sigma_{xxy}|E|^2 + i\sigma_{xyx}|E|^2 = -2i\sigma_{xxy}|E|^2. \tag{31}$$

Here we have used the antisymmetry of the imaginary part of σ with respect to the last two indices. This leads to

$$\sigma_{xxy} = \frac{1}{i\omega}\int [d\boldsymbol{k}]\partial_{k_x}\Omega_z \tag{32}$$

and reproduces the semiclassical formula for σ_{xxy} in Eq. (7). We note that the factor $\tau/(1 - i\omega\tau)$ in the semiclassical formula [Eq. (7)] is replaced by the factor i/ω in the above formula because the $\tau \to \infty$ limit (clean limit) is effectively taken in the Floquet perturbation theory.

Next we study SHG by using Floquet perturbation theory and the two-band model in a similar manner to the CPGE. We consider a system driven by linearly polarized light in the x direction as $E_x(t) = Ee^{-i\omega t} + E^* e^{i\omega t}$ and the SHG in the y direction. The corresponding Floquet Hamiltonian is given by

$$H_F = H_0 + H_1 + H_2, \tag{33}$$

$$(H_0)_{mn} = \begin{pmatrix} \epsilon_v - n\omega & 0 \\ 0 & \epsilon_c - n\omega \end{pmatrix}\delta_{mn}, \tag{34}$$

$$(H_1)_{mn} = (-iA^*\delta_{mn-1} + iA\delta_{mn+1})v_x, \tag{35}$$

$$(H_2)_{mn} = \left(-\frac{(A^*)^2}{2}\delta_{mn-2} + |A|^2\delta_{mn} - \frac{A^2}{2}\delta_{mn+2}\right)\partial_{k_x}v_x. \tag{36}$$

We take $|\psi_{\mathrm{ini}}\rangle = |u_{v,n=0}\rangle$ as the unperturbed wave function and keep the part of the Floquet Hamiltonian within the range $n = -2, \ldots, 2$. The velocity operator along the y direction is given by

$$\begin{aligned}\hat{v_y} &= v_y\delta_{mn} + (-iA^*\delta_{mn-1} + iA\delta_{mn+1})\partial_{k_x}v_y \\ &\quad + \left(-\frac{(A^*)^2}{2}\delta_{mn-2} + |A|^2\delta_{mn} - \frac{A^2}{2}\delta_{mn+2}\right)\partial_{k_x}^2 v_y.\end{aligned} \tag{37}$$

By using Eq. (20), we obtain the Fourier component of the current $J_y = \int [d\boldsymbol{k}] j_y$ proportional to $e^{-2i\omega t}$ as

$$j_y^{(2\omega)} = \sum_n \{\mathrm{tr}[|\psi\rangle\langle\psi|\hat{v_y}]\}_{n+2,n}$$
$$= -2i\frac{E^2}{i\omega}\frac{\partial}{\partial k_x}\left[\frac{\mathrm{Im}[(v_x)_{vc}(v_y)_{cv}]}{(\epsilon_v-\epsilon_c)^2}\right] = i\frac{E^2}{\omega}\partial_{k_x}\Omega_z. \quad (38)$$

Here we have again used the fact that the contributions proportional to E^2/ω^2 vanish due to the TRS and, also, dropped contributions with higher powers of ω. The above expression indicates that the nonlinear conductivity tensor σ_{yxx} is written as

$$\sigma_{yxx} = \frac{i}{\omega}\int [d\boldsymbol{k}]\partial_{k_x}\Omega_z. \quad (39)$$

This again reproduces the semiclassical formula for σ_{yxx} in Eq. (7).

We can extend the above analysis based on the Floquet formalism to general cases with many bands and obtain the same Berry curvature dipole formula. We sketch the derivation in the following (for details, see the Appendix). We consider the general Floquet Hamiltonian under light irradiation, which is given by

$$H_F = H_0 + H_1 + H_2, \quad (40)$$

with

$$H_1 = \sum_i A_i v_i, \quad H_2 = \frac{1}{2}\sum_{i,j} A_i A_j \partial_{k_i} v_j, \quad (41)$$

where H_0 represents a static Hamiltonian with many bands. Using the Floquet perturbation theory in Eq. (19) and the expression for the current in Eq. (20), we obtain the general expression for the nonlinear current response as

$$J_r = -\sum_{i,j} A_i A_j \int [d\boldsymbol{k}]\Bigg[\sum_{n,g}[f(\epsilon_n)-f(\epsilon_g)]\left(\frac{1}{2}\frac{(v_r)_{ng}\left(\partial_{k_i}v_j\right)_{gn}}{\epsilon_n-(\epsilon_g+2\omega)} + \frac{(\partial_r v_j)_{ng}(v_i)_{gn}}{\epsilon_n-(\epsilon_g+\omega)}\right)$$
$$+\sum_{n,g,m}\left(\frac{f(\epsilon_n)}{\epsilon_n-\epsilon_m-\omega} - \frac{f(\epsilon_g)}{\epsilon_g-\epsilon_m+\omega}\right)\frac{(v_r)_{ng}(v_i)_{gm}(v_j)_{mn}}{\epsilon_n-(\epsilon_g+2\omega)}$$
$$+\sum_{n,g,m} f(\epsilon_n)\frac{(v_j)_{nm}(v_r)_{mg}(v_i)_{gn}}{(\epsilon_n-(\epsilon_g+\omega))(\epsilon_n-(\epsilon_m-\omega))} + \sum_n \frac{1}{2} f(\epsilon_n)(\partial_{k_r}\partial_{k_i}v_j)_{nn}\Bigg], \quad (42)$$

with Fermi distribution function $f(\epsilon)$ [where $f(\epsilon_n) = 1(0)$ for occupied (unoccupied) states]. When we expand the current J_r with respect to ω, the lowest order contribution in ω is proportional to ωA^2 in the presence of TRS. In the case of many bands, the Berry curvature dipole for the nth band is written as

$$\partial_{k_i}\Omega_{z,n} = -2\mathrm{Im}\left[\frac{\langle n|\partial_{k_x}H|m\rangle\langle m|\partial_{k_y}H|n\rangle}{(\epsilon_n-\epsilon_m)^2}\right], \quad (43)$$

where n runs over occupied bands and m runs over unoccupied bands. Using this expression for the Berry curvature dipole, it turns out that the lowest order contribution of J_y proportional to ωA^2 is written as

$$J_y = -iwA_x^2\int [d\boldsymbol{k}] f(\epsilon_n)\partial_{k_x}\Omega_{z,n}, \quad (44)$$

which reproduces the Berry curvature dipole formula, Eq. (7), for SHG in the case of many bands. Details of the above calculation for many band cases are described in the Appendix.

To summarize, we derived formulas for the CPGE and SHG in the sufficiently low-frequency region in a fully quantum mechanical way by using the Floquet perturbation theory. This reproduces the semiclassical formula with the Berry curvature dipole.

III. SEMICLASSICAL FORMULAS FOR NONLINEAR OPTICAL EFFECTS

We study nonlinear optical effects in the presence of magnetic fields using the SCA. Deriving semiclassical formulas for nonlinear magneto-optical effects is motivated in the following senses. First, it is theoretically interesting to see how the orbital magnetic moment m, which is the angular momentum of the wave packet and also of geometrical origin, governs nonlinear optical effects and modifies previous semiclassical results for $B = 0$ in Refs. [17] and [18]. Second, the obtained semiclassical formula for nonlinear magnetoconductivity that includes all terms proportional to B^2E is applicable to Weyl semimetals and may explain the directional anisotropy of the magnetoconductivity of Weyl semimetals recently reported in Refs. [10] and [11], which we discuss in Sec. IV. Third, TR-symmetric Weyl semimetals can support large nonlinear Kerr rotation. The intraband contribution to SHG vanishes for $B = 0$ in TR-symmetric Weyl semimetals, and the SHG signal has a contribution linear in B. Thus application of B may lead to giant nonlinear Kerr rotation.

We derive semiclassical formulas for nonlinear magneto-optical effects up to the second order in E. It is convenient to rewrite the equations of motion, (1), to collect time derivatives on the left:

$$\dot{\boldsymbol{r}} = \frac{1}{\hbar D}\left[\nabla_{\boldsymbol{k}}\epsilon_{\boldsymbol{k}} + e\boldsymbol{E}\times\boldsymbol{\Omega}_{\boldsymbol{k}} + \frac{e}{\hbar}(\nabla_{\boldsymbol{k}}\epsilon_{\boldsymbol{k}}\cdot\boldsymbol{\Omega}_{\boldsymbol{k}})\boldsymbol{B}\right], \quad (45)$$

$$\hbar\dot{\boldsymbol{k}} = \frac{1}{D}\left[-e\boldsymbol{E} - \frac{e}{\hbar}\nabla_{\boldsymbol{k}}\epsilon_{\boldsymbol{k}}\times\boldsymbol{B} - \frac{e^2}{\hbar}(\boldsymbol{E}\cdot\boldsymbol{B})\boldsymbol{\Omega}_{\boldsymbol{k}}\right], \quad (46)$$

$$D = 1 + \frac{e}{\hbar}\boldsymbol{B}\cdot\boldsymbol{\Omega}_{\boldsymbol{k}}. \quad (47)$$

The charge density ρ and current density $\boldsymbol{j}$ are given by

$$\rho = -e\int [d\boldsymbol{k}]Df, \tag{48}$$

$$\boldsymbol{j} = -e\int [d\boldsymbol{k}](D\dot{\boldsymbol{r}} + \nabla_{\boldsymbol{r}}\times \boldsymbol{m}_{\boldsymbol{k}})f, \tag{49}$$

with $[d\boldsymbol{k}] = d\boldsymbol{k}/(2\pi)^3$, where the second term of $\boldsymbol{j}$ is a contribution of the magnetization current. We note that the factor D arises from a field-induced change in the volume of the phase space [22]. In the following, we focus on the uniform system. In this case, the expression of the current density reduces to

$$\boldsymbol{j} = -e\int [d\boldsymbol{k}]\left[\tilde{\boldsymbol{v}}_{\boldsymbol{k}} + \frac{e}{\hbar}\boldsymbol{E}\times\boldsymbol{\Omega}_{\boldsymbol{k}} + \frac{e}{\hbar}(\tilde{\boldsymbol{v}}_{\boldsymbol{k}}\cdot\boldsymbol{\Omega}_{\boldsymbol{k}})\boldsymbol{B}\right]f, \tag{50}$$

where we have used

$$\tilde{\boldsymbol{v}}_{\boldsymbol{p}} = \boldsymbol{v}_{\boldsymbol{k}} - (1/\hbar)\nabla_{\boldsymbol{k}}(\boldsymbol{m}\cdot\boldsymbol{B}), \tag{51}$$

with $\boldsymbol{v}_{\boldsymbol{k}} = (1/\hbar)\nabla_{\boldsymbol{k}}\epsilon^0_{\boldsymbol{k}}$.

Now we focus on nonlinear responses driven by monochromatic light with the electric field $\boldsymbol{E}(t) = \boldsymbol{E}e^{-i\omega t}$. We consider current responses at orders E and E^2 as follows. We write the distribution function in Fourier components as

$$f = f_0 + f_1 e^{-i\omega t} + f_2 e^{-2i\omega t}, \tag{52}$$

where f_0 is the unperturbed distribution function and other terms appear in the presence of the electric field of the incident light. The steady-state distribution function is determined by the Boltzmann equation

$$\frac{df}{dt} = \frac{f_0 - f}{\tau}, \tag{53}$$

where

$$\frac{df}{dt} = \dot{\boldsymbol{k}}\cdot\nabla_{\boldsymbol{k}} f + \partial_t f. \tag{54}$$

This gives a recursive equation for the Fourier components f_i. By combining the Fourier components f_i and Eq. (50), we obtain nonlinear current responses in powers of E. In the following, we apply the above SCA to the linear current responses and the second-order nonlinear optical effects in the presence of magnetic fields.

A. Linear current responses

We first study the linear current responses with $\boldsymbol{B}$. We derive the semiclassical formula for the conductivity up to the second order of B in terms of the Berry curvature and orbital magnetic moment.

The current response of the frequency ω is obtained from f_1 in Eq. (52). By equating terms proportional to $e^{-i\omega t}$ in Eq. (54), we obtain

$$\left[-e\boldsymbol{E} - \frac{e^2}{\hbar}(\boldsymbol{E}\cdot\boldsymbol{B})\boldsymbol{\Omega}_{\boldsymbol{k}}\right]\cdot\nabla_{\boldsymbol{p}} f_0 - i\omega f_1 = -\frac{f_1}{\tau}, \tag{55}$$

with $\nabla_{\boldsymbol{p}} = (1/\hbar)\nabla_{\boldsymbol{k}}$, where we have dropped the term involving $(\nabla_{\boldsymbol{k}}\epsilon_{\boldsymbol{k}})\times\boldsymbol{B}$ because it is perpendicular to $\nabla_{\boldsymbol{p}} f_0 = (1/\hbar)(\nabla_{\boldsymbol{k}}\epsilon_{\boldsymbol{k}})\partial_\epsilon f_0$. This leads to

$$f_1 = \frac{-\tau}{1-i\omega\tau}\frac{1}{D}\left[-e\boldsymbol{E} - \frac{e^2}{\hbar}(\boldsymbol{E}\cdot\boldsymbol{B})\boldsymbol{\Omega}_{\boldsymbol{k}}\right]\cdot\nabla_{\boldsymbol{p}} f_0. \tag{56}$$

Now the current response linear in E is given by

$$\begin{aligned}\boldsymbol{j}_1 = \frac{e\tau}{1-i\omega\tau}\int_{\mathrm{BZ}}[d\boldsymbol{k}]\frac{1}{D}\Bigg\{&\left[\tilde{\boldsymbol{v}}_{\boldsymbol{k}} + \frac{e}{\hbar}(\tilde{\boldsymbol{v}}_{\boldsymbol{k}}\cdot\boldsymbol{\Omega}_{\boldsymbol{k}})\boldsymbol{B}\right]\\ &\times\left[-e\boldsymbol{E} - \frac{e^2}{\hbar}(\boldsymbol{E}\cdot\boldsymbol{B})\boldsymbol{\Omega}_{\boldsymbol{k}}\right]\cdot\nabla_{\boldsymbol{p}} f_0 + \frac{e}{\hbar}\boldsymbol{E}\times\boldsymbol{\Omega}_{\boldsymbol{k}} f_0\Bigg\},\end{aligned} \tag{57}$$

where $f_0 = \theta(E_F - \epsilon_{\boldsymbol{k}} - \boldsymbol{m}_{\boldsymbol{k}}\cdot\boldsymbol{B})$ with the step function $\theta(x) = 0 (x<0), 1 (x\geqslant 0)$. This expression is reduced if we focus on the case where the electric field $\boldsymbol{E}$ is applied along the ith direction and the system preserves the TRS in the absence of magnetic fields. Specifically, we consider terms up to $\propto\boldsymbol{B}$ that are nonvanishing with the TRS by expanding as $1/D \simeq 1 + (e/\hbar)\boldsymbol{B}\cdot\boldsymbol{\Omega}_{\boldsymbol{k}}$, which leads to

$$\begin{aligned}\boldsymbol{j}_1 = \frac{e\tau}{1-i\omega\tau}\int_{\mathrm{BZ}}[d\boldsymbol{k}]\Bigg\{&-\boldsymbol{v}_{\boldsymbol{k}} eE(\boldsymbol{v}_{\boldsymbol{k}})_i\partial_\epsilon f_0'\\ &+\frac{e}{\hbar}(\boldsymbol{E}\times\boldsymbol{\Omega}_{\boldsymbol{k}})(\boldsymbol{m}\cdot\boldsymbol{B})\partial_\epsilon f_0'\Bigg\},\end{aligned} \tag{58}$$

with $f_0' = \theta(E_F - \epsilon_{\boldsymbol{k}})$, i.e., a distribution function when $\boldsymbol{B}=0$. Here we have used the fact that ∂_{p_i}, $\boldsymbol{v}_{\boldsymbol{p}}$, $\boldsymbol{\Omega}$, and $\boldsymbol{m}$ are odd under the TRS. The first term in the integral is the metallic conductivity, while the second term describes regular Hall conductivity linear in B (in contrast to anomalous Hall conductivity, which is nonzero in the absence of B). This second term indicates that the orbital magnetic moment gives a semiclassical description related to Landau level formation in the quantum limit. We note that there is no B-linear contribution to the longitudinal conductivity σ_{ii} because the Onsager relation constrains the conductivity as $\sigma_{ij}(B) = \sigma_{ji}(-B)$ and the longitudinal conductivity should be an even function of B.

Next, we derive the formula for the longitudinal magnetoconductance. Its lowest order dependence on B is quadratic due to the Onsager relation. The B^2 contribution to the longitudinal current response is explicitly written as

$$\begin{aligned}\boldsymbol{j}_{B^2} = \frac{e^2\tau}{\hbar}\int_{\mathrm{BZ}}[d\boldsymbol{k}]\Bigg\{&-\frac{e}{\hbar}\boldsymbol{E}\cdot\nabla_{\boldsymbol{k}} f_0(\epsilon^0)[-e(\boldsymbol{v}_{\boldsymbol{k}}\cdot\boldsymbol{\Omega}_{\boldsymbol{k}})(\boldsymbol{B}\cdot\boldsymbol{\Omega}_{\boldsymbol{k}})\boldsymbol{B} - e\boldsymbol{\Omega}_{\boldsymbol{k}}\cdot\nabla_{\boldsymbol{k}}(\boldsymbol{m}\cdot\boldsymbol{B})\boldsymbol{B} + e(\boldsymbol{B}\cdot\boldsymbol{\Omega}_{\boldsymbol{k}})^2\boldsymbol{v}_{\boldsymbol{k}} + (\boldsymbol{B}\cdot\boldsymbol{\Omega}_{\boldsymbol{k}})\nabla_{\boldsymbol{k}}(\boldsymbol{m}\cdot\boldsymbol{B})]\\ &+\left[\frac{1}{\hbar}\boldsymbol{E}\cdot\nabla_{\boldsymbol{k}}\left(\frac{\partial f_0(\epsilon^0)}{\partial\epsilon}\boldsymbol{m}\cdot\boldsymbol{B}\right) - \frac{e}{\hbar}(\boldsymbol{E}\cdot\boldsymbol{B})(\boldsymbol{\Omega}_{\boldsymbol{k}}\cdot\nabla_{\boldsymbol{k}} f_0(\epsilon^0))\right][e(\boldsymbol{v}_{\boldsymbol{k}}\cdot\boldsymbol{\Omega}_{\boldsymbol{k}})\boldsymbol{B} - e(\boldsymbol{B}\cdot\boldsymbol{\Omega}_{\boldsymbol{k}})\boldsymbol{v}_{\boldsymbol{k}} - \boldsymbol{\partial}_{\boldsymbol{k}}(\boldsymbol{m}\cdot\boldsymbol{B})]\\ &+\frac{e}{\hbar}(\boldsymbol{E}\cdot\boldsymbol{B})\left[\boldsymbol{\Omega}_{\boldsymbol{k}}\cdot\boldsymbol{\partial}_{\boldsymbol{k}}\left(\frac{\partial f_0(\epsilon^0)}{\partial\epsilon}\boldsymbol{m}\cdot\boldsymbol{B}\right)\right]\boldsymbol{v}_{\boldsymbol{k}} - \frac{1}{2}\boldsymbol{E}\cdot\boldsymbol{\partial}_{\boldsymbol{k}}\left[\frac{\partial^2 f_0(\epsilon^0)}{\partial\epsilon^2}(\boldsymbol{m}\cdot\boldsymbol{B})^2\right]\boldsymbol{v}_{\boldsymbol{k}}\Bigg\}.\end{aligned} \tag{59}$$

In addition to terms that contribute isotropically to the current density, there are several terms that contribute to the current density specifically along $\boldsymbol{B}$, which results in an anisotropic magnetoconductance if it is applied to Weyl semimetals as we discuss in Sec. IV.

B. Second-order nonlinear optical effects

We move on to the second-order nonlinear optical effects, which include SHG and the photogalvanic effect. We derive the general formulas which are applied to Weyl/Dirac semimetals in Sec. V.

We consider the SHG that is described by the current response of frequency 2ω. By equating terms proportional to $e^{-2i\omega t}$ in the Boltzmann equation, (54), we obtain

$$\frac{1}{D}\left[-e\boldsymbol{E}-\frac{e^2}{\hbar}(\boldsymbol{E}\cdot\boldsymbol{B})\boldsymbol{\Omega}_{\boldsymbol{k}}\right]\cdot\nabla_{\boldsymbol{p}} f_1 - 2i\omega f_2 = -\frac{f_2}{\tau}, \tag{60}$$

which leads to

$$f_2 = \frac{\tau^2}{(1-i\omega\tau)(1-2i\omega\tau)}\frac{1}{D^2}\left\{\left[-e\boldsymbol{E}-\frac{e^2}{\hbar}(\boldsymbol{E}\cdot\boldsymbol{B})\boldsymbol{\Omega}_{\boldsymbol{k}}\right]\cdot\nabla_{\boldsymbol{p}}\right\}^2 f_0. \tag{61}$$

The second-order current response of the frequency 2ω is given by

$$\begin{aligned}
\boldsymbol{j_2} &= -e\int_{\mathrm{BZ}}[d\boldsymbol{k}]\left\{\left[\tilde{\boldsymbol{v}}_{\boldsymbol{k}}+\frac{e}{\hbar}(\tilde{\boldsymbol{v}}_{\boldsymbol{k}}\cdot\boldsymbol{\Omega}_{\boldsymbol{k}})\boldsymbol{B}\right]f_2+\frac{e}{\hbar}(\boldsymbol{E_0}\times\boldsymbol{\Omega})f_1\right\}\\
&= -e\int_{\mathrm{BZ}}[d\boldsymbol{k}]\left\{\left[\tilde{\boldsymbol{v}}_{\boldsymbol{k}}+\frac{e}{\hbar}(\tilde{\boldsymbol{v}}_{\boldsymbol{k}}\cdot\boldsymbol{\Omega}_{\boldsymbol{k}})\boldsymbol{B}\right]\frac{\tau^2}{(1-i\omega\tau)(1-2i\omega\tau)}\frac{1}{D^2}\left\{\left[-e\boldsymbol{E}-\frac{e^2}{\hbar}(\boldsymbol{E}\cdot\boldsymbol{B})\boldsymbol{\Omega}_{\boldsymbol{k}}\right]\cdot\nabla_{\boldsymbol{p}}\right\}^2 f_0\right.\\
&\quad\left.+\frac{e}{\hbar}\boldsymbol{E}\times\boldsymbol{\Omega}_{\boldsymbol{k}}\frac{\tau}{1-i\omega\tau}\frac{1}{D}\left[-e\boldsymbol{E}-\frac{e^2}{\hbar}(\boldsymbol{E}\cdot\boldsymbol{B})\boldsymbol{\Omega}_{\boldsymbol{k}}\right]\cdot\nabla_{\boldsymbol{p}} f_0\right\}.
\end{aligned} \tag{62}$$

Now we focus on the case of linearly polarized light where the electric field is given by $\boldsymbol{E}(t)=Ee^{-i\omega t}\boldsymbol{e_i}$ ($\boldsymbol{e_i}$ being the unit vector along the ith direction) and see how the above general formula can be simplified in several cases by assuming the TRS in the following. First, when $\boldsymbol{B}=\boldsymbol{0}$, Eq. (62) reduces to

$$\boldsymbol{j_2}(B=0) = \frac{-e\tau}{1-i\omega\tau}\int_{\mathrm{BZ}}[d\boldsymbol{k}]\frac{e^2}{\hbar}E_i^2\left(\boldsymbol{e_i}\times\partial_{p_i}\boldsymbol{\Omega}_{\boldsymbol{k}}\right)f_0. \tag{63}$$

This recovers the previously obtained semiclassical formula, Eq. (7), for SHG. The above expression clarifies that the transverse component of the SHG is described by the Berry curvature dipole $\partial_{p_i}\boldsymbol{\Omega}_{\boldsymbol{k}}$. This Berry curvature dipole contribution can be nonzero only when the inversion symmetry is broken since inversion symmetry constrains $\Omega_{\boldsymbol{k}}=\Omega_{-\boldsymbol{k}}$ and causes cancellation of the Berry curvature dipole between $\boldsymbol{k}$ and $-\boldsymbol{k}$ [17,18]. Second, we consider the case where the magnetic field $\boldsymbol{B}$ is nonzero. The application of $\boldsymbol{B}$ leads to rotation of the polarization plane of the SHG, which is known as nonlinear Kerr rotation and is an important nonlinear optical effect. We study the nonlinear Kerr rotation by keeping contributions up to linear in B. We start with the case where $\boldsymbol{E}$ and $\boldsymbol{B}$ are perpendicular to each other ($\boldsymbol{E}\cdot\boldsymbol{B}=0$). The modification $\Delta\boldsymbol{j_2}$ in the first order of B reads

$$\Delta\boldsymbol{j_2} = \frac{-e\tau^2}{(1-i\omega\tau)(1-2i\omega\tau)}\int_{\mathrm{BZ}}[d\boldsymbol{k}]e^2E_i^2\left\{\left[-2\boldsymbol{v}_{\boldsymbol{k}}\left(\frac{e}{\hbar}\boldsymbol{B}\cdot\boldsymbol{\Omega}_{\boldsymbol{k}}\right)-\frac{1}{\hbar}\nabla_{\boldsymbol{k}}(\boldsymbol{m}\cdot\boldsymbol{B})+\frac{e}{\hbar}(\boldsymbol{v}_{\boldsymbol{k}}\cdot\boldsymbol{\Omega}_{\boldsymbol{k}})\boldsymbol{B}\right]\partial_{p_i}^2 f_0' - \left(\partial_{p_i}^2\boldsymbol{v}_{\boldsymbol{k}}\right)(\boldsymbol{m}\cdot\boldsymbol{B})\partial_\epsilon f_0'\right\}. \tag{64}$$

Here we have used $f_0=f_0'+(\boldsymbol{m}\cdot\boldsymbol{B})\partial_\epsilon f_0'$. The nonlinear Kerr rotation arises from the component of $\Delta\boldsymbol{j_2}$ perpendicular to $\boldsymbol{j_2}(B=0)$ and encodes the information on the Berry curvature $\boldsymbol{\Omega}$ and the orbital magnetic moment $\boldsymbol{m}$. We note that the term $\propto(\boldsymbol{v}_{\boldsymbol{k}}\cdot\boldsymbol{\Omega}_{\boldsymbol{k}})\boldsymbol{B}$ vanishes in the case of two-dimensional systems (where $\boldsymbol{v}_{\boldsymbol{p}}\perp\boldsymbol{\Omega}_{\boldsymbol{p}}$). Finally, we consider the case with $\boldsymbol{E}\cdot\boldsymbol{B}\neq 0$. The further modification $\widetilde{\Delta\boldsymbol{j_2}}$ (in addition to $\Delta\boldsymbol{j_2}$) up to the B linear term is given by

$$\widetilde{\Delta\boldsymbol{j_2}} = \frac{e\tau^2}{(1-i\omega\tau)(1-2i\omega\tau)}\frac{1}{D^2}\int_{\mathrm{BZ}}[d\boldsymbol{k}]\frac{e^3}{\hbar}E_i^2B_i\boldsymbol{v}_{\boldsymbol{k}}\left[-2\boldsymbol{\Omega}_{\boldsymbol{k}}\cdot\nabla_{\boldsymbol{p}}\partial_{p_i}-\left(\partial_{p_i}\boldsymbol{\Omega}_{\boldsymbol{k}}\right)\cdot\nabla_{\boldsymbol{p}}\right]f_0'. \tag{65}$$

Next we derive a semiclassical formula for the photogalvanic effect in the presence of B. The PGE causes static dc current in the second order of E. The dc component of the distribution function is also modified at the second order of E as $f_0\to f_0+\delta f_0$. The associated Boltzmann equation is written as

$$\frac{\delta f_0}{\tau} = \left[-e\boldsymbol{E}^*-\frac{e^2}{\hbar}(\boldsymbol{E}^*\cdot\boldsymbol{B})\boldsymbol{\Omega}_{\boldsymbol{k}}\right]\cdot\nabla_{\boldsymbol{p}} f_1, \tag{66}$$

which is solved as

$$\delta f_0 = \frac{\tau^2}{1-i\omega\tau}\left[-e\boldsymbol{E}^* - \frac{e^2}{\hbar}(\boldsymbol{E}^*\cdot\boldsymbol{B})\boldsymbol{\Omega}_{\boldsymbol{k}}\right]\left[-e\boldsymbol{E} - \frac{e^2}{\hbar}(\boldsymbol{E}\cdot\boldsymbol{B})\boldsymbol{\Omega}_{\boldsymbol{k}}\right] f_0. \tag{67}$$

This leads to the dc photovoltaic current $\delta \boldsymbol{j_0}$ given by

$$\begin{aligned}\delta\boldsymbol{j_0} &= -e\int_{\mathrm{BZ}}[d\boldsymbol{k}]\left\{\left[\boldsymbol{v_k} - \frac{1}{\hbar}\nabla_{\boldsymbol{k}}(\boldsymbol{m}\cdot\boldsymbol{B}) + \frac{e}{\hbar}(\boldsymbol{v_k}\cdot\boldsymbol{\Omega_k})\boldsymbol{B}\right]\delta f_0 + \frac{e}{\hbar}(\boldsymbol{E_0}^*\times\boldsymbol{\Omega})f_1\right\}\\ &= -e\int_{\mathrm{BZ}}[d\boldsymbol{k}]\left\{\left[\boldsymbol{v_k} - \frac{1}{\hbar}\nabla_{\boldsymbol{k}}(\boldsymbol{m}\cdot\boldsymbol{B}) + \frac{e}{\hbar}(\boldsymbol{v_k}\cdot\boldsymbol{\Omega_k})\boldsymbol{B}\right]\frac{\tau^2}{1-i\omega\tau}\frac{1}{D^2}\left\{\left[-e\boldsymbol{E} - \frac{e^2}{\hbar}(\boldsymbol{E}\cdot\boldsymbol{B})\boldsymbol{\Omega_k}\right]\cdot\nabla_{\boldsymbol{p}}\right\}^2 f_0\right.\\ &\quad\left. + \frac{e}{\hbar}\boldsymbol{E}\times\boldsymbol{\Omega_k}\frac{\tau}{1-i\omega\tau}\frac{1}{D}[-e\boldsymbol{E} - e^2(\boldsymbol{E}\cdot\boldsymbol{B})\boldsymbol{\Omega_k}]\cdot\nabla_{\boldsymbol{p}} f_0\right\},\end{aligned} \tag{68}$$

where we write $\boldsymbol{E}^* = \boldsymbol{E}$ in the second line, for simplicity. This expression is analogous to $\boldsymbol{j_2}$ (i.e., SHG) and indicates that the Berry curvature and the orbital magnetic moment of the Bloch bands also govern the Hall angle of dc photocurrent in the presence of an external magnetic field $\boldsymbol{B}$.

IV. ANGLE-DEPENDENT MAGNETORESISTANCE

In this section, we study MR by using the SCA developed in the previous section. In particular, we focus on the current response $J \propto EB^2$ and study how the Berry curvature and the orbital magnetic moment contribute to MR in Weyl semimetals, since the interplay of these two quantities in the transport properties of Weyl semimetals has not been fully investigated except in a few studies [8,9,23,24]. The obtained angle dependence of magnetoresistance is compared with recent magnetotransport experiments for Dirac semimetals [10,11].

We consider the Hamiltonian for Weyl semimetals given by

$$H = \eta v_F \boldsymbol{\sigma}\cdot\boldsymbol{p}, \tag{69}$$

where v_F is the Fermi velocity and $\eta = \pm 1$ specifies the chirality. In this case, the velocity operator, the Berry curvature, and the orbital magnetic moment are written as

$$\boldsymbol{v_k} = v_F\hat{\boldsymbol{k}}, \tag{70}$$

$$\boldsymbol{\Omega} = -\eta\frac{1}{2k^2}\hat{\boldsymbol{k}}, \tag{71}$$

$$\boldsymbol{m} = -\eta\frac{ev_F}{2k}\hat{\boldsymbol{k}} \tag{72}$$

for the conduction band, where $\hat{k}$ denotes the unit vector along $\boldsymbol{k}$.

Now we apply the semiclassical formula, Eq. (59), for the linear current response $\boldsymbol{j_1}$ proportional to B^2 to Weyl semimetals and study the angle-dependent MR. First, we suppose that the electric field is applied in the z direction as $\boldsymbol{E} = E\boldsymbol{e}_z$, where $\boldsymbol{e}_z$ denotes the unit vector along the z direction. In this case, the current along the z direction $(j_1)_z$ is given by

$$(j_1)_z = \frac{1}{6\pi^2\hbar}\tau e^2 v_F k_F^2 E + \frac{1}{30\pi^2\hbar^3 k_F^2}\tau e^4 v_F B^2 E \tag{73a}$$

when $\boldsymbol{E} \parallel \boldsymbol{B}$ and

$$(j_1)_z = \frac{1}{6\pi^2\hbar}\tau e^2 v_F k_F^2 E - \frac{1}{60\pi^2\hbar^3 k_F^2}\tau e^4 v_F B^2 E \tag{73b}$$

when $\boldsymbol{E} \perp \boldsymbol{B}$ (e.g., $\boldsymbol{B} \parallel \hat{x}$), where we have assumed $\tau\omega \ll 1$. Here, the first term is the isotropic dc conductivity and the second term is an anisotropic correction which originates from the $\boldsymbol{E}\cdot\boldsymbol{B}$ term related to the chiral anomaly in Weyl semimetals. The second term accounts for the negative MR when $\boldsymbol{E} \parallel \boldsymbol{B}$ and the positive MR when $\boldsymbol{E} \perp \boldsymbol{B}$. Thus the semiclassical theory for the linear conductivity including the effects of both $\boldsymbol{\Omega}$ and $\boldsymbol{m}$ captures the directional anisotropy of linear conductivity in the $\boldsymbol{B}$ field, which is usually considered to be evidence of a Weyl fermion in transport measurements.

Next we discuss the full angle dependence of the current response in the magnetic field. When the electric field is applied in the direction tilted by θ from the direction of the magnetic field $\boldsymbol{B}$, the longitudinal magnetoconductivity $\sigma(B)$ is given by

$$\frac{\sigma(B) - \sigma(B=0)}{\sigma(B=0)} = \frac{-1 + 3\cos^2\theta}{10}\frac{e^2 B^2}{\hbar^2 k_F^4}. \tag{74}$$

Equation (74) does not depend on the chirality of the Weyl node or on the band in which the chemical potential is located. It shows that the MR is positive when $\boldsymbol{E} \perp \boldsymbol{B}$ and decreases to negative as $\theta \to 0$. If we separately look at contributions to the MR from the Berry curvature and the orbital magnetic moment, we find that either the Berry curvature or the orbital magnetic moment alone gives a negative MR [Figs. 2(a) and 2(b)], while the interplay between the Berry curvature and the orbital magnetic moment gives a positive MR [Fig. 2(c)]. As a whole, Eq. (74) gives the angular dependences as shown in Fig. 2(d). We note that the anisotropic magnetoconductance in the semiclassical formula Eq. (74) is not solely described by the contribution from the chiral anomaly. Specifically, the contribution from the chiral anomaly discussed in Ref. [25] is found in the term

$$\frac{-e^4\tau}{\hbar}\int_{\mathrm{BZ}}[d\boldsymbol{k}](\boldsymbol{\Omega_k}\cdot\nabla_{\boldsymbol{p}} f_0(\epsilon^0))(\boldsymbol{v_k}\cdot\boldsymbol{\Omega_k})(\boldsymbol{E}\cdot\boldsymbol{B})\boldsymbol{B} \tag{75}$$

in Eq. (59) and gives a negative MR in Weyl semimetals. In contrast, there are several terms involving the orbital magnetic moment which lead to contributions of opposite signs.

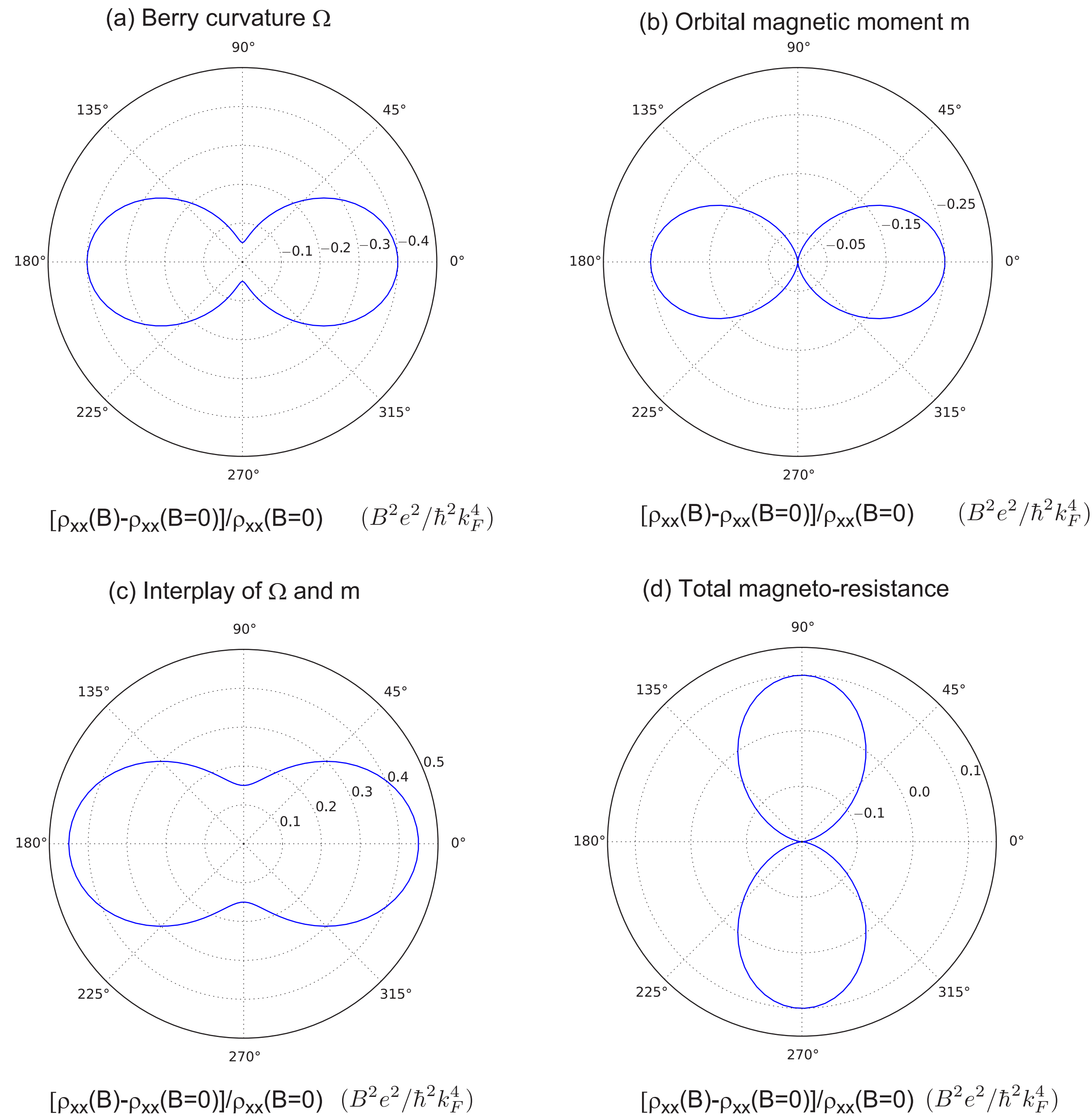

FIG. 2. Angle dependence of longitudinal magnetoresistance (LMR) for Weyl semimetals derived from the semiclassical approach [Eq. (59)]. Blue lines are polar plots of the LMR $[\rho_{xx}(B) - \rho_{xx}(B = 0)]/\rho_{xx}(B = 0)$ as a function of the relative angle θ between $\boldsymbol{E}$ and $\boldsymbol{B}$. We show angle dependences of contributions to the LMR from (a) the Berry curvature, (b) the orbital magnetic moment, (c) the interplay between the Berry curvature and the orbital magnetic moment, and (d) the total angle dependence of the LMR.

A similar angular dependence of the MR from Eq. (74) in the weak-field region has been observed in magnetotransport experiments on Dirac semimetals [10,11]. In particular, Ref. [11] reported that the sign change of the MR occurs around 45° in the low-B region for the Dirac semimetal Na_3Bi, which is consistent with our semiclassical result shown in Fig. 2(d). We note that our calculation for Weyl semimetals is also applicable to Dirac semimetals with the mild assumption that the degenerate energy bands having opposite chirality in Dirac semimetals are decoupled from each other.

Finally, we present estimates for the above nonlinear conductivities derived for Weyl semimetals. The directional anisotropy of the linear conductivity is given by the ratio of the two terms $\propto B^0$ and $\propto B^2$ in Eq. (73). The anisotropy ratio amounts to $0.06(B/1\,\mathrm{T})^2$ for typical parameters $v_F = 3 \times 10^5$ m/s and $E_F = 10$ meV for the Weyl semimetal material, TaAs [26,27].

V. NONLINEAR MAGNETO-OPTICAL RESPONSES IN WEYL SEMIMETALS

In this section, we study the nonlinear optical responses of Weyl semimetals in the presence of a magnetic field. Specifically, we study the second harmonic generation and the nonlinear Kerr rotation with B and discuss the fact that Weyl semimetals can support large nonlinear Kerr rotation in the infrared regime.

First, we note that SHG is vanishing in the absence of magnetic fields when the Weyl fermion has a linear and isotropic dispersion as in Eq. (69). The contribution from the Berry curvature dipole to the SHG cancels within the Weyl node after k integration. Thus, the application of $\boldsymbol{B}$ is necessary in order for the SHG to be nonvanishing for isotropic Weyl fermions. In this sense, SHG with B in Weyl semimetals is a fundamental nonlinear optical effect which is related to the monopole structure in the momentum space via the orbital magnetic moment.

Now we consider the SHG of Weyl fermions in the presence of a uniform magnetic field applied to the z direction [$\boldsymbol{B} = (0,0,B)$] and study the nonlinear current response proportional to B. When the electric field is perpendicular to $\boldsymbol{B}$, e.g., $\boldsymbol{E} = (E,0,0)$, the nonlinear current response is given by

$$\boldsymbol{j_2} = \left(0,0,\frac{e^4 v_F B}{60\pi^2\hbar^3\omega^2 k_F}E^2\right), \tag{76}$$

where we have assumed $\tau\omega \gg 1$ by focusing on the high-frequency regime. On the other hand, when the electric field is applied in the z direction [$\boldsymbol{E} = (0,0,E)$] and is parallel to $\boldsymbol{B}$, there is an additional contribution to SHG from the $\boldsymbol{E}\cdot\boldsymbol{B}$ term related to the chiral anomaly of Weyl fermions. In this case we obtain

$$\boldsymbol{j_2} = \left(0,0,\frac{2e^4 v_F B}{15\pi^2\hbar^3\omega^2 k_F}E^2\right). \tag{77}$$

This expression shows an enhancement of the SHG compared to the case of $\boldsymbol{E} \perp \boldsymbol{B}$; the chiral anomaly enhances the SHG. Since $\boldsymbol{j_2} \propto k_F^{-1}$, the contribution to SHG proportional to B becomes very large when the Fermi energy is close to the Weyl point. This enhancement is a consequence of the divergence of the Berry curvature and orbital magnetic moment near the Weyl point. In this regard, the SHG of Weyl semimetals under B is tied to the monopole physics in the momentum space described by the Berry curvature. In practice, these divergences are cut off by the energy broadening due to the nonzero relaxation time τ. This cutoff takes place around $k_F \simeq 1/(v_F\tau)$. In addition, there is another cutoff that depends on the strength of the electric field E. Since semiclassical treatment for Weyl fermions is only valid when $eE\tau/\hbar < k_F$ (otherwise interband effects become relevant because the shift of wave number exceeds the Fermi wave number), the divergence is also cut off around $k_F \simeq eE\tau/\hbar$.

The enhancement of SHG in Weyl semimetals can be detected as a large Kerr rotation signal. In the case of a general band structure, SHG can become nonzero even for $B = 0$ if we include the effect of band bending, e.g., by introducing a k^2 term in H. This nonzero contribution to the SHG for $B = 0$ is, in general, not parallel to the above B-linear contribution to the SHG. Therefore, when the magnetic field is applied, the diverging B-linear contribution to SHG parallel to $\boldsymbol{B}$ leads to a large rotation of the polarization angle of SHG and, hence, a large nonlinear Kerr rotation. Incidentally, we note that when higher order terms with respect to k are present in the Hamiltonian such as k^2 terms, additional terms having higher powers in k_F arise in the current response in Eq. (77). However, when the Fermi energy is close to the Weyl point and k_F is small enough, these corrections become negligible.

Finally, we estimate the magnitude of the nonlinear magneto-optical susceptibility, which is given by $\chi \equiv j_2/(i\omega)\epsilon_0 E^2$. For the photon energy $\hbar\omega = 0.1$ eV in the infrared region, the nonlinear susceptibility is estimated as $|\chi| = 1500 \times (B/1\ \mathrm{T})$pm/V from Eq. (77) by adopting the parameters, $v_F = 3\times 10^5$ m/s and $E_F = 10$ meV for the Weyl semimetal material TaAs. For comparison, GaAs, which is a representative SHG medium, shows nonlinear susceptibility of $\chi \simeq 500$ pm/V in the visible-light region [28]. Thus Weyl semimetals potentially support large nonlinear Kerr rotation from the Fermi surface effect for low photon energies. Since a recent optical measurement in TaAs reported giant SHG signals in the visible-light region [29], Weyl semimetals are considered to be interesting nonlinear optical media in a wide range of frequency.

VI. DISCUSSION

We have studied the CPGE and SHG in the low-frequency limit from a fully quantum mechanical treatment using Floquet perturbation theory. By doing so, we have reproduced the expressions with the Berry curvature dipole that were previously obtained from semiclassics. While we have focused on second-order nonlinear optical effects in this paper, the Floquet perturbation theory provides a systematic way to study general nonlinear optical responses in the low-frequency limit. Thus it will be an interesting issue to apply this method to other higher order nonlinear optical effects and investigate their geometrical meaning.

We have derived semiclassical formulas for the magnetoconductance and nonlinear magneto-optical effects by taking into account the orbital magnetic moment. There is an effort to partially incorporate interband effects in the SCA [30]. Applying this method to isotropic Weyl fermions with a linear dispersion does not lead to any correction to our semiclassical formulas for magnetoconductance and SHG derived in Secs. IV and V. However, in the case of a general band dispersion, the interband contributions will generate correction terms which are proportional to some inverse powers of the energy band separation. Moreover, complete formulas for these nonlinear optical effects can be derived by using a quantum mechanical treatment. The quantum treatment may be feasible for two-band systems like we employed to deduce quantum formulas for the CPGE and SHG, while it should become very complicated in cases of a general number of bands. In particular, it will be interesting to see how the Berry curvature and orbital magnetic moment arise in the quantum mechanical treatment, as is possible for linear responses for an arbitrary number of bands [8,9], and what the corrections from the semiclassical formulas look like. These issues are left as future problems.

There exists another class of Weyl semimetals in which Weyl points are created by applying magnetic fields and breaking time-reversal symmetry artificially in centrosymmetric crystals. Such creation of Weyl semimetals with a B field was recently reported in GdPtBi [31,32], and semiclassical analysis of magnetoresistance for these materials has been performed in Ref. [33]. It would also be interesting to apply our semiclassical formula to nonlinear magneto-optical/transport properties in these field-created Weyl semimetals.

ACKNOWLEDGMENTS

We thank M. Kolodrubetz, B. M. Fregoso, and L. Wu for fruitful discussions. This work was supported by the Gordon and Betty Moore Foundation's EPiQS Initiative Theory Center Grant (T.M.), NSF Grant No. DMR-1507141 (S.Z.), the Gordon and Betty Moore Foundation's EPiQS Initiative through Grant No. GBMF4537 (J.O.), and the DOE Quantum Materials program of Lawrence Berkeley National Laboratory, with travel support from the Simons Foundation (J.E.M.).

APPENDIX: DERIVATION OF THE BERRY CURVATURE DIPOLE FORMULA FOR GENERAL BANDS

In this Appendix, we apply the Floquet perturbation theory to systems with a general number of bands and derive the formula for SHG in terms of the Berry curvature dipole. The derivation proceeds in a similar manner to the two-band case presented in Sec. II B but involves more band indices.

We consider a system irradiated with monochromatic light which is described by the time-dependent Hamiltonian

$$\widetilde{H}(t) = H(\vec{p} + e\vec{A}(t)) = H^0 + H^1 + H^2 + \dots = H + \sum_i \big(\partial_{k_i} H\big) e A_i e^{-i\omega t} + \sum_{i,j} \frac{1}{2}\big(\partial_{k_i}\partial_{k_j} H\big) e^2 A_i A_j e^{-2i\omega t} + \dots, \tag{A1}$$

where $H^0 \equiv H$ is the static Hamiltonian in the absence of driving, and $\vec{A}(t) = \vec{A}e^{-i\omega t}$ is the vector potential. For the time-periodic Hamiltonian $\widetilde{H}(t)$, the Floquet Hamiltonian is defined by

$$(H_F)_{mn} = \frac{1}{T}\int_0^T dt e^{i(m-n)\Omega t}\widetilde{H}(t) - n\hbar\Omega\delta_{mn}, \tag{A2}$$

with Floquet indices m and n. In the following, we adopt a simplified notation where we write contributions $H^i(t)$ to the Floquet Hamiltonian H_F just as H^i.

The standard perturbation theory gives the wave function for the perturbed Floquet Hamiltonian H_F as

$$|\psi_{\tilde{n}}\rangle = |\tilde{n}\rangle + \sum_{\tilde{g}\neq\tilde{n}} \frac{H^1_{\tilde{g}\tilde{n}}}{\epsilon_{\tilde{n}} - \epsilon_{\tilde{g}}}|\tilde{g}\rangle + \sum_{\substack{\tilde{n}\neq\tilde{m}\\ \tilde{g}\neq\tilde{n}}} \left[\frac{H^1_{\tilde{g}\tilde{m}}H^1_{\tilde{m}\tilde{n}}}{(\epsilon_{\tilde{n}}-\epsilon_{\tilde{m}})(\epsilon_{\tilde{n}} - \epsilon_{\tilde{g}})} - \frac{H^1_{\tilde{n}\tilde{n}}H^1_{\tilde{g}\tilde{n}}}{(\epsilon_{\tilde{n}} - \epsilon_{\tilde{g}})^2} + \frac{H^2_{\tilde{g}\tilde{n}}}{\epsilon_{\tilde{n}} - \epsilon_{\tilde{g}}}\right]|\tilde{g}\rangle, \tag{A3}$$

where $|\tilde{n}\rangle$ is the unperturbed wave function satisfying $H|\tilde{n}\rangle = \epsilon_{\tilde{n}}|\tilde{n}\rangle$, and $\tilde{n}$ labels the set of the band index and the Floquet index. Here we note that $H^1_{\tilde{n}\tilde{n}} = 0$ in the present case. The explicit form of the wave function ψ_n with band index n and any Floquet index (say, 0) is given by

$$|\psi_n\rangle = |n\rangle + e\sum_{n,g}\frac{\big(\partial_{k_i} H A_i\big)_{gn}}{\epsilon_n - (\epsilon_g + \omega)}|g\rangle + \frac{1}{2}e^2\sum_{n,g}\frac{\big(\partial_{k_i}\partial_{k_j} H A_i A_j\big)_{gn}}{\epsilon_n - (\epsilon_g + 2\omega)}|g\rangle + e^2\sum_{n,m,g}\left[\frac{\big(\partial_{k_j} H A_j\big)_{gm}\big(\partial_{k_i} H A_i\big)_{mn}}{(\epsilon_n - (\epsilon_m + \omega))(\epsilon_n - (\epsilon_g + 2\omega))}\right]|g\rangle, \tag{A4}$$

where $|n\rangle$ denotes the static wave function with band index n, ϵ_n denotes the static energy dispersion with band index n, and $\mathcal{O}_{m,n} = \langle m|\mathcal{O}|n\rangle$.

Now we consider the current response in the α direction, given by

$$J_\alpha(t) = -e\sum_n f(\epsilon_n)\sum_{m',n'}\{\mathrm{tr}[|\psi_{(n,0)}\rangle\langle\psi_{(n,0)}|\hat{v}_\alpha]\}_{m'n'}e^{-i(m'-n')\omega t}, \tag{A5}$$

where $|\psi_{(n,0)}\rangle$ is the perturbed wave function with band index n and Floquet index 0, and m' and n' denote the Floquet indices. The Fermi distribution function $f(\epsilon)$ is given by $f(\epsilon_n) = 1$ for occupied bands and $f(\epsilon_n) = 0$ for unoccupied bands. Since we consider the low-frequency limit where optical transition does not take place, we can assume that the occupation of the perturbed states coincides with that of the unperturbed states. The operator $\hat{v}$ is the Floquet representation of the time-dependent velocity operator $v(t)$, which is given by

$$(\hat{v}_i)_{m'n'} = \frac{1}{T}\int_0^T dt e^{i(m'-n')\omega t}v_i(t) \tag{A6}$$

$$v_i(t) = v_i^0 + v_i^1 + v_i^2 + \dots = \partial_{k_i} H + \sum_j \big(\partial_{k_i}\partial_{k_j} H\big) e A_j e^{-i\omega t} + \sum_{i,j}\frac{1}{2}\big(\partial_{k_i}\partial_{k_j}\partial_{k_l} H\big) e^2 A_j A_l e^{-2i\omega t} + \dots. \tag{A7}$$

For the real external field $\vec{A}(t) = \vec{A}e^{-i\omega t} + \vec{A}e^{i\omega t}$, we obtain the second-order current response J_r along the r direction, which is proportional to $e^{-i2\omega t}$, as

$$\begin{aligned} J_r = -e^3 \sum_{i,j} A_i A_j \int [d\boldsymbol{k}] \sum_{n,g} \Bigg[& \frac{1}{2} f(\epsilon_n) \frac{\left(\partial_{k_i}\partial_{k_j} H\right)_{gn}}{\epsilon_n - (\epsilon_g + 2\omega)} \langle n|\partial_{k_r} H|g\rangle + \frac{1}{2} f(\epsilon_n) \frac{\left(\partial_{k_i}\partial_{k_j} H\right)_{ng}}{\epsilon_n - (\epsilon_g - 2\omega)} \langle g|\partial_{k_r} H|n\rangle \\ & + \sum_m \frac{f(\epsilon_n)}{\epsilon_n - \epsilon_m - \omega} \frac{\left(\partial_{k_j} H\right)_{gm}\left(\partial_{k_i} H\right)_{mn}}{\epsilon_n - (\epsilon_g + 2\omega)} \langle n|\partial_{k_r} H|g\rangle + \sum_m \frac{f(\epsilon_n)}{\epsilon_n - \epsilon_m + \omega} \frac{\left(\partial_{k_i} H\right)_{nm}\left(\partial_{k_j} H\right)_{mg}}{\epsilon_n - (\epsilon_g - 2\omega)} \langle g|\partial_{k_r} H|n\rangle \\ & + f(\epsilon_n) \frac{\left(\partial_{k_i} H\right)_{gn}}{\epsilon_n - (\epsilon_g + \omega)} \langle n|\partial_{k_r}\partial_{k_j} H|g\rangle + f(\epsilon_n) \frac{\left(\partial_{k_i} H\right)_{ng}}{\epsilon_n - (\epsilon_g - \omega)} \langle g|\partial_{k_r}\partial_{k_j} H|n\rangle \\ & + \sum_m f(\epsilon_n) \frac{\left(\partial_{k_i} H\right)_{gn}}{\epsilon_n - (\epsilon_g + \omega)} \frac{\left(\partial_{k_j} H\right)_{nm}}{\epsilon_n - (\epsilon_m - \omega)} \langle m|\partial_{k_r} H|g\rangle + \frac{1}{2} f(\epsilon_n) \langle n|\partial_{k_r}\partial_{k_i}\partial_{k_j} H|n\rangle \Bigg]. \end{aligned} \tag{A8}$$

This expression can be rewritten as

$$\begin{aligned} J_r = -e^3 \sum_{i,j} A_i A_j \int [d\boldsymbol{k}] \sum_n \Bigg[& \sum_g \frac{1}{2}(f(\epsilon_n) - f(\epsilon_g)) \frac{\langle n|\partial_{k_r} H|g\rangle\langle g|\partial_{k_i}\partial_{k_j} H|n\rangle}{\epsilon_n - (\epsilon_g + 2\omega)} \\ & + \sum_{m,g} \left(\frac{f(\epsilon_n)}{\epsilon_n - \epsilon_m - \omega} - \frac{f(\epsilon_g)}{\epsilon_g - \epsilon_m + \omega} \right) \frac{\langle n|\partial_{k_r} H|g\rangle\langle g|\partial_{k_i} H|m\rangle\langle m|\partial_{k_j} H|n\rangle}{\epsilon_n - (\epsilon_g + 2\omega)} \\ & + \sum_g (f(\epsilon_n) - f(\epsilon_g)) \frac{\langle n|\partial_{k_r}\partial_{k_j} H|g\rangle\langle g|\partial_{k_i} H|n\rangle}{\epsilon_n - (\epsilon_g + \omega)} \\ & + \sum_{m,g} f(\epsilon_n) \frac{\langle n|\partial_{k_j} H|m\rangle\langle m|\partial_{k_r} H|g\rangle\langle g|\partial_{k_i} H|n\rangle}{(\epsilon_n - (\epsilon_g + \omega))(\epsilon_n - (\epsilon_m - \omega))} + \frac{1}{2} f(\epsilon_n)\langle n|\partial_{k_r}\partial_{k_i}\partial_{k_j} H|n\rangle \Bigg]. \end{aligned} \tag{A9}$$

Since we are interested in the intraband effects in the low-frequency limit (ω much smaller than the band gap), we expand the current J_r in terms of ω as $J_r = J_r^0 + J_r^1 + J_r^2 + \ldots$, with $J_r^n \propto \omega^n$. The lowest order term in ω is the zeroth-order term, which is given by

$$\begin{aligned} J_r^0 = -e^3 \sum_{i,j} A_i A_j \int [d\boldsymbol{k}] \sum_n \Bigg[& \sum_g \frac{1}{2}(f(\epsilon_n) - f(\epsilon_g)) \frac{\langle n|\partial_{k_r} H|g\rangle\langle g|\partial_{k_i}\partial_{k_j} H|n\rangle}{\epsilon_n - \epsilon_g} \\ & + \sum_{m,g}{}' \left(\frac{f(\epsilon_n)}{\epsilon_n - \epsilon_m} - \frac{f(\epsilon_g)}{\epsilon_g - \epsilon_m} \right) \frac{\langle n|\partial_{k_r} H|g\rangle\langle g|\partial_{k_i} H|m\rangle\langle m|\partial_{k_j} H|n\rangle}{\epsilon_n - \epsilon_g} + \sum_g{}' (f(\epsilon_n) - f(\epsilon_g)) \frac{\langle n|\partial_{k_r}\partial_{k_j} H|g\rangle\langle g|\partial_{k_i} H|n\rangle}{\epsilon_n - \epsilon_g} \\ & + \sum_{m,g}{}' f(\epsilon_n) \frac{\langle n|\partial_{k_j} H|m\rangle\langle m|\partial_{k_r} H|g\rangle\langle g|\partial_{k_i} H|n\rangle}{(\epsilon_n - \epsilon_g)(\epsilon_n - \epsilon_m)} - 2\sum_g{}' f(\epsilon_n) \frac{\langle n|\partial_{k_r} H|g\rangle\langle g|\partial_{k_i} H|n\rangle\langle n|\partial_{k_j} H|n\rangle}{(\epsilon_n - \epsilon_g)^2} \\ & - 2\sum_g{}' f(\epsilon_g) \frac{\langle n|\partial_{k_r} H|g\rangle\langle g|\partial_{k_i} H|g\rangle\langle g|\partial_{k_j} H|n\rangle}{(\epsilon_n - \epsilon_g)^2} + \sum_m{}' f(\epsilon_n) \frac{\langle n|\partial_{k_j} H|m\rangle\langle m|\partial_{k_r} H|n\rangle\langle n|\partial_{k_i} H|n\rangle}{(\epsilon_n - \epsilon_m)^2} \\ & + \sum_g{}' f(\epsilon_n) \frac{\langle n|\partial_{k_j} H|n\rangle\langle n|\partial_{k_r} H|g\rangle\langle g|\partial_{k_i} H|n\rangle}{(\epsilon_n - \epsilon_g)^2} + \frac{1}{2} e^2 f(\epsilon_n)\langle n|\partial_{k_r}\partial_{k_i}\partial_{k_j} H|n\rangle \Bigg]. \end{aligned} \tag{A10}$$

Here $\sum_g'$ ($\sum_{m,g}'$) denotes the summation where the band index g (m,g) runs over those that do not set the denominator to 0. We note that the fifth to eighth terms are obtained by setting one energy denominator to be $1/\omega$ and expanding the other energy denominator up to ω^2 in the second and the fourth terms in Eq. (A9). In addition, the time reversal symmetry, $\mathcal{T} = K$, leads to the symmetry properties of the Hamiltonian and its eigenstates given by

$$H(k) = H(-k), \quad \epsilon(k) = \epsilon(-k), \quad |n(k)\rangle = \langle n(-k)|. \tag{A11}$$

By using these properties that hold in the presence of TRS, we find that the above expression for J_r^0 vanishes at the zeroth order. Therefore, the lowest order term is actually the first-order term J_r^1.

The first-order term in ω is written as

$$
\begin{aligned}
J_r = -e^3\omega \sum_{i,j} A_i A_j \int [d\boldsymbol{k}] \sum_n \Bigg[& \sum_g{}' (f(\epsilon_n) - f(\epsilon_g)) \frac{\langle n|\partial_{k_r} H|g\rangle\langle g|\partial_{k_i}\partial_{k_j} H|n\rangle}{(\epsilon_n-\epsilon_g)^2} \\
& + 2\sum_{m,g}{}' \left(\frac{f(\epsilon_n)}{\epsilon_n-\epsilon_m} - \frac{f(\epsilon_g)}{\epsilon_g-\epsilon_m}\right) \frac{\langle n|\partial_{k_r} H|g\rangle\langle g|\partial_{k_i} H|m\rangle\langle m|\partial_{k_j} H|n\rangle}{(\epsilon_n-\epsilon_g)^2} \\
& + \sum_{m,g}{}' \left(\frac{f(\epsilon_n)}{(\epsilon_n-\epsilon_m)^2} + \frac{f(\epsilon_g)}{(\epsilon_g-\epsilon_m)^2}\right) \frac{\langle n|\partial_{k_r} H|g\rangle\langle g|\partial_{k_i} H|m\rangle\langle m|\partial_{k_j} H|n\rangle}{\epsilon_n-\epsilon_g} - 4\sum_g{}' f(\epsilon_n) \frac{\langle n|\partial_{k_r} H|g\rangle\langle g|\partial_{k_i} H|n\rangle\langle n|\partial_{k_j} H|n\rangle}{(\epsilon_n-\epsilon_g)^3} \\
& - 4\sum_g{}' f(\epsilon_g) \frac{\langle n|\partial_{k_r} H|g\rangle\langle g|\partial_{k_i} H|g\rangle\langle g|\partial_{k_j} H|n\rangle}{(\epsilon_n-\epsilon_g)^3} + \sum_g{}' (f(\epsilon_n) - f(\epsilon_g)) \frac{\langle n|\partial_{k_r}\partial_{k_j} H|g\rangle\langle g|\partial_{k_i} H|n\rangle}{(\epsilon_n-\epsilon_g)^2} \\
& - \sum_m{}' f(\epsilon_n) \frac{\langle n|\partial_{k_j} H|m\rangle\langle m|\partial_{k_r} H|n\rangle\langle n|\partial_{k_i} H|n\rangle}{(\epsilon_n-\epsilon_m)^3} + \sum_g{}' f(\epsilon_n) \frac{\langle n|\partial_{k_j} H|n\rangle\langle n|\partial_{k_r} H|g\rangle\langle g|\partial_{k_i} H|n\rangle}{(\epsilon_n-\epsilon_g)^3} \\
& - \sum_{m,g}{}' f(\epsilon_n) \frac{\langle n|\partial_{k_j} H|m\rangle\langle m|\partial_{k_r} H|g\rangle\langle g|\partial_{k_i} H|n\rangle}{(\epsilon_n-\epsilon_g)(\epsilon_n-\epsilon_m)^2} + \sum_{m,g}{}' f(\epsilon_n) \frac{\langle n|\partial_{k_j} H|m\rangle\langle m|\partial_{k_r} H|g\rangle\langle g|\partial_{k_i} H|n\rangle}{(\epsilon_n-\epsilon_g)^2(\epsilon_n-\epsilon_m)} \Bigg].
\end{aligned} \tag{A12}
$$

By using the properties from the TRS, this can be reduced as

$$
\begin{aligned}
J_r = -2e^3\omega \sum_{i,j} A_i A_j \int [d\boldsymbol{k}] \sum_n f(\epsilon_n) & \\
\times \Bigg[\sum_g{}' f(\epsilon_n) \frac{\langle n|\partial_{k_r} H|g\rangle\langle g|\partial_{k_i}\partial_{k_j} H|n\rangle}{(\epsilon_n-\epsilon_g)^2} & + 2\sum_{m,g}{}' \frac{1}{\epsilon_n-\epsilon_m} \frac{\langle n|\partial_{k_r} H|g\rangle\langle g|\partial_{k_i} H|m\rangle\langle m|\partial_{k_j} H|n\rangle}{(\epsilon_n-\epsilon_g)^2} \\
+ \sum_{m,g}{}' \frac{1}{(\epsilon_n-\epsilon_m)^2} \frac{\langle n|\partial_{k_r} H|g\rangle\langle g|\partial_{k_i} H|m\rangle\langle m|\partial_{k_j} H|n\rangle}{\epsilon_n-\epsilon_g} & - 3\sum_g{}' \frac{\langle n|\partial_{k_r} H|g\rangle\langle g|\partial_{k_i} H|n\rangle\langle n|\partial_{k_j} H|n\rangle}{(\epsilon_n-\epsilon_g)^3} \\
+ \sum_g{}' \frac{\langle n|\partial_{k_r}\partial_{k_j} H|g\rangle\langle g|\partial_{k_i} H|n\rangle}{(\epsilon_n-\epsilon_g)^2} & - \sum_{m,g}{}' \frac{\langle n|\partial_{k_j} H|m\rangle\langle m|\partial_{k_r} H|g\rangle\langle g|\partial_{k_i} H|n\rangle}{(\epsilon_n-\epsilon_g)(\epsilon_n-\epsilon_m)^2} \Bigg].
\end{aligned} \tag{A13}
$$

Now let us consider the specific case relevant to the Berry curvature dipole formula. Namely, we suppose that E is applied along the x direction and consider the current J in the y direction:

$$
\begin{aligned}
J_y = -2e^3\omega A_x A_x \int [d\boldsymbol{k}] \sum_n f(\epsilon_n) & \\
\times \Bigg[\sum_g{}' f(\epsilon_n) \frac{\langle n|\partial_{k_y} H|g\rangle\langle g|\partial_{k_x}\partial_{k_x} H|n\rangle}{(\epsilon_n-\epsilon_g)^2} & + 2\sum_{m,g}{}' \frac{1}{\epsilon_n-\epsilon_m} \frac{\langle n|\partial_{k_y} H|g\rangle\langle g|\partial_{k_x} H|m\rangle\langle m|\partial_{k_x} H|n\rangle}{(\epsilon_n-\epsilon_g)^2} \\
-3\sum_g{}' \frac{\langle n|\partial_{k_y} H|g\rangle\langle g|\partial_{k_x} H|n\rangle\langle n|\partial_{k_x} H|n\rangle}{(\epsilon_n-\epsilon_g)^3} & + \sum_{m,g}{}' \frac{1}{(\epsilon_n-\epsilon_m)^2} \frac{\langle n|\partial_{k_y} H|g\rangle\langle g|\partial_{k_x} H|m\rangle\langle m|\partial_{k_x} H|n\rangle}{\epsilon_n-\epsilon_g} \\
+ \sum_g{}' \frac{\langle n|\partial_{k_y}\partial_{k_x} H|g\rangle\langle g|\partial_{k_x} H|n\rangle}{(\epsilon_n-\epsilon_g)^2} & - \sum_{m,g}{}' \frac{\langle n|\partial_{k_x} H|m\rangle\langle m|\partial_{k_y} H|g\rangle\langle g|\partial_{k_x} H|n\rangle}{(\epsilon_n-\epsilon_g)(\epsilon_n-\epsilon_m)^2} \Bigg].
\end{aligned} \tag{A14}
$$

The $\boldsymbol{k}$ integral of the Berry curvature dipole $\Omega_{z,n}$ for the nth band is explicitly written in many-band systems as

$$
\begin{aligned}
& \int [d\boldsymbol{k}] \partial_x \Omega_{z,n}(k) \\
& = -2\partial_x \int [d\boldsymbol{k}] \, \mathrm{Im}[\langle \partial_x n|\partial_y n\rangle] = i\partial_x \int [d\boldsymbol{k}] \sum_g [\langle \partial_x n|g\rangle\langle g|\partial_y n\rangle - \langle \partial_y n|g\rangle\langle g|\partial_x n\rangle] \\
& = i\partial_x \int [d\boldsymbol{k}] \sum_g{}' \left[\frac{\langle n|\partial_x H|g\rangle\langle g|\partial_y H|n\rangle}{(\epsilon_n-\epsilon_g)^2} - \frac{\langle n|\partial_y H|g\rangle\langle g|\partial_x H|n\rangle}{(\epsilon_n-\epsilon_g)^2} \right]
\end{aligned}
$$

$$
\begin{aligned}
&= -2i\int[d\boldsymbol{k}]\sum_g{}' \bigg[\frac{\langle n|\partial_y H|g\rangle\langle\partial_x g|\partial_x H|n\rangle}{(\epsilon_n-\epsilon_g)^2}+\frac{\langle n|\partial_y H|g\rangle\langle g|\partial_x\partial_x H|n\rangle}{(\epsilon_n-\epsilon_g)^2}+\frac{\langle n|\partial_y H|g\rangle\langle g|\partial_x H|\partial_x n\rangle}{(\epsilon_n-\epsilon_g)^2}+\frac{\langle\partial_x n|\partial_y H|g\rangle\langle g|\partial_x H|n\rangle}{(\epsilon_n-\epsilon_g)^2}\\
&\quad+\frac{\langle n|\partial_x\partial_y H|g\rangle\langle g|\partial_x H|n\rangle}{(\epsilon_n-\epsilon_g)^2}+\frac{\langle n|\partial_y H|\partial_x g\rangle\langle g|\partial_x H|n\rangle}{(\epsilon_n-\epsilon_g)^2}-2\frac{\langle n|\partial_y H|g\rangle\langle g|\partial_x H|n\rangle}{(\epsilon_n-\epsilon_g)^3}[(v_x)_{nn}-(v_x)_{gg}]\bigg]\\
&= -2i\int[d\boldsymbol{k}]\sum_g{}' \bigg[\frac{\langle n|\partial_y H|g\rangle\langle g|\partial_x\partial_x H|n\rangle}{(\epsilon_n-\epsilon_g)^2}+\frac{\langle n|\partial_x\partial_y H|g\rangle\langle g|\partial_x H|n\rangle}{(\epsilon_n-\epsilon_g)^2}-2\frac{\langle n|\partial_y H|g\rangle\langle g|\partial_x H|n\rangle}{(\epsilon_n-\epsilon_g)^3}[(v_x)_{nn}-(v_x)_{gg}]\bigg]\\
&\quad+\sum_{g,m}{}'\bigg[-\frac{\langle n|\partial_y H|g\rangle\langle g|\partial_x H|m\rangle\langle m|\partial_x H|n\rangle}{(\epsilon_m-\epsilon_g)(\epsilon_n-\epsilon_g)^2}+\frac{\langle n|\partial_y H|g\rangle\langle g|\partial_x H|m\rangle\langle m|\partial_x H|n\rangle}{(\epsilon_n-\epsilon_m)(\epsilon_n-\epsilon_g)^2}\\
&\quad-\frac{\langle n|\partial_x H|m\rangle\langle m|\partial_y H|g\rangle\langle g|\partial_x H|n\rangle}{(\epsilon_m-\epsilon_n)(\epsilon_n-\epsilon_g)^2}+\frac{\langle n|\partial_y H|g\rangle\langle g|\partial_x H|m\rangle\langle m|\partial_x H|n\rangle}{(\epsilon_m-\epsilon_g)(\epsilon_n-\epsilon_m)^2}\bigg],
\end{aligned}
\tag{A15}
$$

where we have used the TRS to simplify the expressions and the equation $\langle n|\partial_k m\rangle = \langle n|v|m\rangle/(\epsilon_m-\epsilon_n)$. We note that the region of the above $\boldsymbol{k}$ integration can be any $\mathcal{T}$-symmetric region that includes both $\boldsymbol{k}$ and $-\boldsymbol{k}$, especially, the Fermi sea satisfying $f(\epsilon_n)=1$.

By using Eq. (A15), we finally obtain

$$
\begin{aligned}
J_y &= -2e^3\omega A_x A_x\int[d\boldsymbol{k}]\sum_n f(\epsilon_n)\\
&\quad\times\bigg[\frac{\partial_x\Omega_{z,n}}{-2i}+\sum_g{}'\frac{\langle n|\partial_y H|g\rangle\langle g|\partial_x H|n\rangle\langle n|\partial_x H|n\rangle}{(\epsilon_n-\epsilon_g)^3}+\sum_g{}'\frac{1}{(\epsilon_n-\epsilon_g)^2}\frac{\langle n|\partial_{k_y}H|g\rangle\langle g|\partial_{k_x}H|g\rangle\langle g|\partial_{k_x}H|n\rangle}{\epsilon_n-\epsilon_g}\\
&\quad+\sum_g{}'\frac{1}{\epsilon_n-\epsilon_g}\frac{\langle n|\partial_{k_y}H|g\rangle\langle g|\partial_{k_x}H|g\rangle\langle g|\partial_{k_x}H|n\rangle}{(\epsilon_n-\epsilon_g)^2}-3\sum_g{}'\frac{\langle n|\partial_{k_y}H|g\rangle\langle g|\partial_{k_x}H|n\rangle\langle n|\partial_{k_x}H|n\rangle}{(\epsilon_n-\epsilon_g)^3}\\
&\quad+2\sum_g{}'\frac{\langle n|\partial_y H|g\rangle\langle g|\partial_x H|n\rangle}{(\epsilon_n-\epsilon_g)^3}[(v_x)_{nn}-(v_x)_{gg}]\bigg]\\
&= -ie^3\omega A_x A_x\int[d\boldsymbol{k}]\partial_x\Omega_z.
\end{aligned}
\tag{A16}
$$

This indicates that the nonlinear conductivity for the SHG is given by

$$
\sigma_{yxx} = \frac{ie^3}{\omega}\int[d\boldsymbol{k}]\sum_n f(\epsilon_n)\partial_{k_x}\Omega_{z,n},
\tag{A17}
$$

which reproduces Eq. (44) in Sec. II B and proves the Berry curvature dipole formula for SHG in general cases with many bands.

[1] D. J. Thouless, Phys. Rev. B **27**, 6083 (1983).
[2] R. D. King-Smith and D. Vanderbilt, Phys. Rev. B **47**, 1651 (1993).
[3] X.-L. Qi, T. L. Hughes, and S.-C. Zhang, Phys. Rev. B **78**, 195424 (2008).
[4] A. M. Essin, J. E. Moore, and D. Vanderbilt, Phys. Rev. Lett. **102**, 146805 (2009).
[5] A. M. Essin, A. M. Turner, J. E. Moore, and D. Vanderbilt, Phys. Rev. B **81**, 205104 (2010).
[6] A. Malashevich, I. Souza, S. Coh, and D. Vanderbilt, New J. Phys. **12**, 053032 (2010).
[7] N. Nagaosa, J. Sinova, S. Onoda, A. H. MacDonald, and N. P. Ong, Rev. Mod. Phys. **82**, 1539 (2010).
[8] S. Zhong, J. E. Moore, and I. Souza, Phys. Rev. Lett. **116**, 077201 (2016).
[9] J. Ma and D. A. Pesin, Phys. Rev. B **92**, 235205 (2015).
[10] T. Liang, Q. Gibson, M. N. Ali, M. Liu, R. J. Cava, and N. P. Ong, Nat. Mater. **14**, 280 (2014).
[11] J. Xiong, S. K. Kushwaha, T. Liang, J. W. Krizan, M. Hirschberger, W. Wang, R. J. Cava, and N. P. Ong, Science **350**, 413 (2015).
[12] G. Sundaram and Q. Niu, Phys. Rev. B **59**, 14915 (1999).
[13] N. Ashcroft and N. Mermin, *Solid State Physics* (Saunders College, Philadelphia, 1976).
[14] S. D. Ganichev, E. L. Ivchenko, S. N. Danilov, J. Eroms, W. Wegscheider, D. Weiss, and W. Prettl, Phys. Rev. Lett. **86**, 4358 (2001).
[15] H. Diehl, V. A. Shalygin, V. V. Bel'kov, C. Hoffmann, S. N. Danilov, T. Herrle, S. A. Tarasenko, D. Schuh, C. Gerl, W. Wegscheider, W. Prettl, and S. D. Ganichev, New J. Phys. **9**, 349 (2007).

[16] P. Olbrich, S. A. Tarasenko, C. Reitmaier, J. Karch, D. Plohmann, Z. D. Kvon, and S. D. Ganichev, Phys. Rev. B **79**, 121302 (2009).
[17] J. E. Moore and J. Orenstein, Phys. Rev. Lett. **105**, 026805 (2010).
[18] I. Sodemann and L. Fu, Phys. Rev. Lett. **115**, 216806 (2015).
[19] T. Morimoto and N. Nagaosa, Science Advances **2**, e1501524 (2016).
[20] S. Kohler, J. Lehmann, and P. Hänggi, Phys. Rep. **406**, 379 (2005).
[21] T. Oka and H. Aoki, Phys. Rev. B **79**, 081406 (2009).
[22] D. Xiao, J. Shi, and Q. Niu, Phys. Rev. Lett. **95**, 137204 (2005).
[23] F. M. D. Pellegrino, M. I. Katsnelson, and M. Polini, Phys. Rev. B **92**, 201407 (2015).
[24] D. Varjas, A. G. Grushin, R. Ilan, and J. E. Moore, arXiv:1607.05278.
[25] D. T. Son and B. Z. Spivak, Phys. Rev. B **88**, 104412 (2013).
[26] H. Weng, C. Fang, Z. Fang, B. A. Bernevig, and X. Dai, Phys. Rev. X **5**, 011029 (2015).
[27] X. Huang, L. Zhao, Y. Long, P. Wang, D. Chen, Z. Yang, H. Liang, M. Xue, H. Weng, Z. Fang, X. Dai, and G. Chen, Phys. Rev. X **5**, 031023 (2015).
[28] S. Bergfeld and W. Daum, Phys. Rev. Lett. **90**, 036801 (2003).
[29] L. Wu, S. Patankar, T. Morimoto, N. L. Nair, E. Thewalt, A. Little, J. G. Analytis, J. E. Moore, and J. Orenstein, Nat. Phys. (2016), doi:10.1038/nphys3969.
[30] Y. Gao, S. A. Yang, and Q. Niu, Phys. Rev. Lett. **112**, 166601 (2014).
[31] M. Hirschberger, S. Kushwaha, Z. Wang, Q. Gibson, C. A. Belvin, B. A. Bernevig, R. J. Cava, and N. P. Ong, Nat. Mater. **15**, 1161 (2016).
[32] C. Shekhar, A. K. Nayak, S. Singh, N. Kumar, S.-C. Wu, Y. Zhang, A. C. Komarek, E. Kampert, Y. Skourski, J. Wosnitza, W. Schnelle, A. McCollam, U. Zeitler, J. Kubler, S. S. P. Parkin, B. Yan, and C. Felser, arXiv:1604.01641.
[33] J. Cano, B. Bradlyn, Z. Wang, M. Hirschberger, N. P. Ong, and B. A. Bernevig, arXiv:1604.08601.